The epigenomic landscape of single vascular cells reflects developmental origin and identifies disease risk loci

Chad S. Weldy, M.D., Ph.D.[1,2], Paul P. Cheng, M.D., Ph.D.[1,3], Wenduo Guo, Ph.D.[1], Albert J. Pedroza, M.D.[4], Alex R. Dalal, M.D.[4], Matthew D. Worssam, Ph.D.[1], Disha Sharma, Ph.D.[1], Trieu Nguyen, B.S.[1], Ramendra Kundu, Ph.D.[1], Michael P. Fischbein, M.D., Ph.D.[3,4], Thomas Quertermous, M.D.[1,3, #]

[1]Department of Medicine, Division of Cardiovascular Medicine, Stanford University

[2]Stanford Center for Inherited Cardiovascular Disease

[3]Stanford Cardiovascular Institute, Stanford University

[4]Department of Cardiothoracic Surgery, Stanford University

Running title: Epigenomic landscape of single vascular cells

[#]To whom correspondence should be addressed:

Thomas Quertermous, M.D.

Falk CVRC, Rm 265

300 Pasteur Drive

Stanford, CA 94305

Tel: 650-723-5012

Email: tomq1@stanford.edu

Abstract

Rationale: Vascular beds have distinct susceptibility to atherosclerosis and aneurysm, yet the biological underpinnings of vascular bed specific disease risk are largely unknown. Vascular tissues have different developmental origins which may influence global chromatin accessibility. Understanding chromatin accessibility and gene expression profiles on single cell resolution is crucial to gain insight into vascular bed specific disease risk.

Objective: We aim to understand, at single cell resolution, the global chromatin accessibility and gene expression profiles across distinct vascular beds in the healthy adult mouse to provide insight into the potential mechanisms of vascular bed specific disease risk.

Methods and Results: We performed single cell chromatin accessibility (scATACseq) and gene expression profiling (scRNAseq) of healthy adult mouse vascular tissue from three vascular beds, 1) aortic root and ascending aorta, 2) brachiocephalic and carotid artery, and 3) descending thoracic aorta. By integrating datasets and comparing vascular beds within cell type, we identified thousands of differentially accessible chromatin peaks within smooth muscle cells, fibroblasts, and endothelial cells, demonstrating numerous enhancers to be vascular bed specific. We revealed an epigenetic 'memory' of embryonic origin with differential chromatin accessibility of key developmental transcription factors such as *Tbx20*, *Hand2*, *Gata4*, and *Hoxb* family members. Increased transcription factor motif accessibility in ascending fibroblasts compared to descending further highlights SMAD2/3 functions and suggests a differential susceptibility to TGFβ. By isolating primary adventitial fibroblasts from

ascending and descending thoracic aorta from adult mice, we demonstrate ascending fibroblasts to have a distinctly higher transcriptional response to TGFβ compared to descending fibroblasts, highlighting that distinct chromatin accessibility between vascular beds is retained following primary *in vitro* culture and influences responsiveness to disease relevant signaling.

Conclusions: This work supports a paradigm that the epigenomic and transcriptional landscapes of vascular cells are cell type and vascular bed specific and that differentially accessible regions are enriched for disease risk genes.

Introduction

The risk to develop vascular disease is vascular bed specific — a clinical observation that has been well described for over a half century,[1-3] yet the biological mechanisms by which this occurs remain poorly understood. Smooth muscle cells (SMC), fibroblasts, and endothelial cells which make up vascular tissues have distinct developmental origins[4-10] and this embryonic lineage diversity has been hypothesized to contribute to vascular bed specific susceptibility to disease.[5] Genome wide association studies (GWAS) of vascular disease have revealed unique loci for disease in individual vascular beds, highlighting differential genetic and molecular etiologies for disease in differing vascular tissues.[11-17] Understanding the fundamental mechanisms which mediate this differential susceptibility to disease is critical to understand mechanisms of vascular disease and discover novel therapeutic targets.

Genomic structure and chromatin accessibility within the cell is intricately linked to function and governs transcriptional programs that drive disease risk.[18] This context is important when considering that heritability of complex disease is determined by common genetic variation that largely mediates disease risk through modifying genomic enhancer function within regions of open chromatin.[19] The recent advancement of single cell global chromatin accessibility profiling through *A*ssay for *T*ransposase *A*ccessible *C*hromatin *seq*uencing (scATACseq) in combination with single cell transcriptomic analysis (scRNAseq) has further indicated that genetic risk of cardiac[20, 21] and vascular disease[22-24] is driven in part through modification of cell type specific enhancers regulating expression of disease modifying genes in a cell type specific manner.

During vasculogenesis in early life, the carotid arteries and great vessels of the heart form from the pharyngeal arch arteries which appear in a craniocaudal sequence and then regress or remodel to form a definitive vascular pattern.[25-28] The adult murine aorta is composed of vascular cells from diverse embryonic origin including the secondary heart field, neural crest, and somitic mesoderm[5] and reside in spatially distinct domains.[8] Further, analysis of smooth

muscle cells from adult healthy vascular tissue in mouse has shown a differential gene expression profile across vascular beds which suggests relevance to vascular bed specific disease risk.[29]

Epigenomic landscape of tissues may be influenced by embryonic origin, yet cell type specific enhancers of vascular tissues between vascular beds have yet to be mapped. By performing scATACseq combined with scRNAseq of healthy adult mouse aortic tissue from three vascular beds, 1) aortic root and ascending aorta, 2) brachiocephalic and carotid artery, and 3) descending thoracic aorta — representing the secondary heart field and neural crest, neural crest, and somitic mesoderm, respectively — we report that cell type specific enhancers of vascular cells are vascular bed specific, demonstrate a developmental "memory", and are related to disease risk genes. We reveal key differential chromatin accessibility of transcription factor motifs between vascular beds, and through isolation and *in* vitro culture of primary adventitial fibroblasts from murine ascending and descending aorta, further reveal this differential chromatin accessibility to have functional consequence regarding response to TGFβ. This work provides important insights into disease risk across vascular beds and supports the concept that the epigenomic landscape of vascular tissues is vascular bed specific and influences disease risk.

Methods

Data Availability

All data and materials are being deposited to the National Center for Biotechnology Information Gene Expression Omnibus and will be available for general public access.

Mice and Micro-Dissections

Male 14-16-week-old C57Bl/6 mice were purchased from Jackson Laboratory (Bar Harbor, ME). The animal study protocol was approved by the Administrative Panel on Laboratory Animal

Care at Stanford University and procedures were followed in accordance with institutional guidelines.

Mice were anesthetized with isoflurane and sacrificed with cervical dislocation technique. Vascular tissue was flushed with injection of 5mL of phosphate buffered saline (PBS) into the left ventricle after an incision was made at the right atrium. Aortic tissue was dissected including the aortic root and ascending aorta up to the take-off of the brachiocephalic artery. The brachiocephalic artery and its extension into the right common carotid artery were carefully dissected under stereoscope. The descending thoracic aorta was then isolated from past the left subclavian artery down to the renal arteries.

Vascular Tissue Dissociation, Cell Capture, and Sequencing

Tissues were collected and dissociated for single cell capture as previously described.[22, 30, 31] Briefly, vascular tissue was washed three times in PBS, tissues were then placed into an enzymatic dissociation cocktail (2□U□ml−1 Liberase (5401127001; Sigma–Aldrich) and 2□U□ml−1 elastase (LS002279; Worthington) in Hank's Balanced Salt Solution (HBSS)), and minced. After incubation at 37□°C for 1□h, the cell suspension was strained and then pelleted by centrifugation at 500g for 5□min. The enzyme solution was then discarded, and cells were resuspended in fresh HBSS. To increase biological replication, 8 mice were used to obtain single-cell suspensions for each vascular tissue (aortic root/ascending aorta, brachiocephalic/carotid, and descending thoracic aorta). Cells were FACS sorted and live cells were identified as previously described.[31] Briefly, cells were sorted on a BD Aria II instrument, where cells were gated on forward/side scatter parameters to exclude small debris and then gated on forward scatter height versus forward scatter area to exclude obvious doublet events. Approximately 100-150,000 live cells were sorted for each vascular bed, where a portion of cells were taken directly to scRNAseq capture. For single cell ATAC, cells were

collected in BSA-coated tubes, and nuclei isolated per 10X recommended protocol, and captured on the 10X scATAC platform.

All single-cell capture and library preparation was performed at the Stanford Genomic Sequencing Service Center. Cells were loaded into a 10x Genomics microfluidics chip and encapsulated with barcoded oligo-dT-containing gel beads using the 10x Genomics Chromium controller according to the manufacturer's instructions. Single-cell libraries were then constructed according to the manufacturer's instructions (Illumina). Libraries from individual samples were multiplexed into one lane before sequencing on an Illumina platform with targeted depth of 50,000 reads per cell for RNA and 75,000 reads/cell for ATAC. Post filtering for non-cells, mean number of reads within peaks per cell in scATAC data was 18,000-20,000 as was seen in our prior report.[22]

Analysis of Single-Cell Sequencing Data

scRNAseq

Fastq files from each vascular bed were aligned to the reference genome (mm10) individually using CellRanger Software (10x Genomics). Individual datasets were aggregated using the CellRanger aggr command without subsampling normalization. The aggregated dataset was then analyzed using the R package Seurat.[32] The dataset was trimmed of cells expressing fewer than 1000 genes, and genes expressed in fewer than 50 cells. The number of genes, number of unique molecular identifiers and percentage of mitochondrial genes were examined to identify outliers. As an unusually high number of genes can result from a 'doublet' event, in which two different cell types are captured together with the same barcoded bead, cells with >6000 genes were discarded. Cells containing >7.5% mitochondrial genes were presumed to be of poor quality and were also discarded. The gene expression values then underwent library-size normalization and normalized using established Single-Cell Transform function in Seurat. No additional batch correction was performed. Principal component analysis was used for

dimensionality reduction, followed by clustering in principal component analysis space using a graph-based clustering approach via Louvain algorithm. UMAP was then used for two-dimensional visualization of the resulting clusters. Analysis, visualization and quantification of gene expression and generation of gene module scores were performed using Seurat's built-in function such as "FeaturePlot", "VlnPlot", "AddModuleScore", and "FindMarker."

scATACseq

Fastq files from each vascular bed were aligned to the reference ATAC genome (mm10) individually using CellRanger Software (10x Genomics). Individual datasets were aggregated using the CellRanger aggr command without subsampling normalization. The aggregated dataset was then analyzed using the R package Signac.[32] The dataset was first trimmed of cells containing fewer than 1000 peaks, and peaks found in fewer than 10 cells. The subsequent cells were then again filtered based off TSS enrichment, nucleosome signal, and percent of reads that lies within peaks found within the larger dataset. Cells with greater than 20,000 reads within peaks or fewer than 3000 peaks, <2 transcription start site (TSS) enrichment, or <15% reads within peaks were removed as they are likely poor-quality nuclei. The remaining cells were then processed using RunTFIDF(), RunSVD() functions from Signac to allow for latent semantic indexing (LSI) of the peaks,[33, 34] which was then used to create UMAPs. Differentially accessible peaks between different populations of cells were found using FindMarker function, using number of peaks as latent variable to correct for depth. Motif matrix was obtained from JASPAR 2020, aligned onto BSgenome.Mmusculus.UCSC.mm10. Accessibility analysis around transcription factor motifs was performed using ChromVar.[35] Merging of scRNA and ATAC data was performed using Pseudo-expression of each gene created using scATACseq GeneActivity function to assign peaks to nearest genes expressed in the scRNA dataset, and mapped onto each other using Canonical Correlation Analysis.

Primary adventitial fibroblast culture and bulk RNA sequencing

We isolated the aortic root and ascending aorta from 6, 12 week old male C57/BL6 mice as well as the descending thoracic aorta to the level of the renal arteries and carefully separated the media from the adventitia by gentle traction with forceps. Adventitia was cut into small pieces with microscissors and plated into 12 well plates with DMEM media with 5% FBS. Following cell attachment to the plate, cells were cultured at 37C and expanded for 48 hours. Cells were washed with PBS and passaged 1x and plated into a 12 well plate at 65,000 cells/mL. Upon cell culture reaching ~80% confluence, cells were treated with either solute control or mouse TGFβ (invitae) (10ng/mL) for 48 hours. Following 48hr treatment, RNA was isolated using Qiagen RNeasy kits and RNA/cDNA library was sequenced with 250M paired end reads. Fastq files were aligned to MM10 murine genome and raw read count and expression normalization was performed with featureCounts[36] and DEseq2,[37] respectively. Differential predicted transcription factor motif accessibility from bulk RNAseq analysis of the 200bp upstream of the transcription start site (TSS) from differentially expressed genes was performed with Hypergeometric Optimization of Motif EnRichment (HOMER).[38]

Results

Single cell analysis of vascular tissue reveals cell type and vascular bed specific epigenomic profiles

We performed microdissections to collect the vascular tissues from three vascular beds in 8 healthy adult C57Bl/6 mice (14-16 weeks of age) including the 1) ascending aorta and aortic root, 2) brachiocephalic and right common carotid arteries, and 3) descending thoracic aorta (Figure 1A). Tissues were pooled by vascular bed, underwent enzymatic digestion and mechanical dissociation, live cells were FACS sorted, and cells were then partitioned for either scRNAseq or for subsequent nuclei isolation and scATACseq using 10X genomics platform as previously described.[22, 30, 31] A total of 21,299 cells and 22,773 cells were profiled with

scRNAseq and scATACseq respectively with roughly 6,000-9,000 cells per vascular bed and sequencing modality. Following quality control and removal of low-quality cells, data was normalized and underwent linear dimensional reduction following standard protocols in R packages Seurat and Signac.[32] Visualization with UMAP methodology for both scRNAseq and scATACseq datasets was performed (Figure 1B&C). UMAP visualization of scRNAseq and scATACseq data reveals a specific pattern where vascular bed origin distinguishes cell clusters (Figure 1B&C).

Given the interrelationship between RNA expression and global chromatin accessibility, these datasets were then integrated together as previously described.[22, 32] Integrated scRNAseq and scATACseq datasets underwent additional non-linear dimensional reduction and UMAP visualization (Figure 1D). The integrated UMAP representing both transcriptomic and chromatin accessibility visually reveals significant differences between cell types by vascular bed (Figure 1D). Analysis of RNA expression of canonical genes to differentiate cell type shows strong correlation to overall gene chromatin activity (e.g. *Myh11* — smooth muscle, Figure 1E&F). Integrated cell clusters were then assigned to the major cell types of the vascular wall, vascular smooth muscle cells (SMCs), fibroblasts, endothelial cells, and macrophages (Figure 1G), using known lineage markers. Further unbiased clustering was performed showing 13 distinct cell clusters (Figure 1H). Of these cell clusters, smooth muscle cells tended to cluster by vascular bed (i.e. ascending, descending, carotid), with two unique ‘nonspecific’ SMC clusters which were composed of cells from each vascular bed at an equal level. Fibroblast clustering shows a specific fibroblast cluster composed of fibroblasts from the ascending aorta, with three ‘nonspecific’ fibroblast clusters (Figure 1H). To further focus on SMC and fibroblast cell populations, a subsetted analysis of SMC and fibroblasts was performed with UMAP visualization demonstrating clear separation of cells by original vascular bed, demonstrating a unique vascular bed specific chromatin and RNA profile by cell type (Figure 1I&J).

Epigenomic patterns of vascular SMCs are cell type and vascular bed specific

UMAP clustering of SMCs from integrated data demonstrates a pattern where SMCs from the ascending aorta, carotid artery, and descending thoracic vascular beds are distinct from one another (Figure 1I). Chromatin peak accessibility analysis between ascending and descending thoracic aorta SMCs identifies 2,304 peaks which are differentially accessible (Figure 2A). Peak locations were analyzed using Genomic Regions Enrichment of Annotations Tool (GREAT).[39] GREAT performs genomic region-gene associations by assigning a regulatory domain for each gene, and then each genomic region is associated with all genes whose regulatory domain it overlaps. Of these peaks, the majority (1,981/2,304; 86%) are associated with 2 genes within a region (Figure 2A, Supplemental Table 1). A distribution of region-gene association distances to TSS is observed where the majority of peaks lie downstream of the TSS (Figure 2B). Roughly 10% of peaks are within 5kb of the TSS of a gene (Figure 2B) and approximately 37% (1596/4280) of region-gene associations are within 50kb of a TSS (Figure 2C).

When comparing peak accessibility between ascending and descending aorta, specific chromatin regions are identified as having marked differential accessibility. A top differentially accessible peak lies at Chr8-57328475-57329393, 7951bp downstream from the TSS for *Hand2* (heart and neural crest derivatives expressed 2) (Figure 2D&E). Coverage plot of SMC chromatin accessibility demonstrates an open chromatin state for this, as well as other, enhancers in this region from the ascending aorta and carotid artery, while they are in closed chromatin states in the descending aorta (Figure 2D). Simultaneous RNA expression analysis reveals a strong association between *Hand2* expression and chromatin accessibility of peak chr8-57328475-57329393 (Figure 2E&F). Top peaks which have increased accessibility within the descending aorta include genomic regions which lie near the *Hoxb* family of transcription factors (Figure 2G, Supplemental Table 1). Consistent with the role of Hox genes during the development of somites, there is an increased chromatin accessibility in Hox genes in the SMCs isolated from the descending aorta in comparison to either ascending aorta or carotid artery

(Figure 2G). The feature plot of a peak near *Hoxb6* located at chr11-96298623-96299539 best demonstrates this contrast between descending aorta SMCs and ascending/carotid SMCs (Figure 2H). Top differential peak analysis reveals other cardiac and vascular development genes which have higher chromatin accessibility within the ascending aorta include *Tbx20*, *Tbx2*, *Gata4*, and *Wnt16*, while homeobox genes such as the *Hoxa/b/c* family of genes, *Smad2*, and *Pax1* are identified as having higher chromatin accessibility within the descending aorta (Supplemental Table 1).

Gene expression analysis using FindMarker from scRNAseq data of SMCs reveals 306 genes which have differential expression among vascular beds (77 ascending, 152 carotid, 76 descending) (Supplemental Tables 2, 3, & 4) which largely match genes which are identified by differential peak analysis (Figure 2I). Top differentially expressed genes within the ascending SMC population includes expected developmental genes such as *Tbx20* and *Hand2*, but also numerous genes with previously demonstrated roles in atherosclerosis suggesting vascular bed specific disease risk mechanisms (Figure 2I, Supplemental Table 2). These genes include *Ccn3* (cellular communication network factor 3) which has previously reported vascular protective effects by inhibiting neointimal formation and plaque development;[40, 41] *Dcn* (decorin), which has been shown to be protective in atherosclerosis;[42] *Col14a1* (collagen type XIV alpha 1 chain) which has increased expression in human atherosclerotic plaque;[43] and *Tns1* (tensin 1) a previously identified CAD GWAS gene.[44] Notably, we identify specific vascular development and inflammation genes as having higher expression within SMCs isolated from the carotid artery, such as *Junb* (junb proto-oncogene) (Figure 2J, Supplemental Table 3), *Atf3* (activating transcription factor 3), and *Egr1* (early growth response 1). *Junb* has specific roles in mediating cellular and arterial contractility,[45] *Atf3* is a CAD GWAS gene and has recently been identified to have vascular protective effect in atherosclerosis,[23] and *Egr1* has critical roles in mediating proinflammatory gene expression and promotes atherosclerosis.[46] Specific genes which have higher expression within the descending thoracic SMCs include signal transduction genes such

as *Rgs5* (Regulator of G protein signaling 5) (Figure 2K, Supplemental Table 4), *Fn1* (fibronectin 1), and *Ccdc3* (coiled-coil domain containing 3). *Rgs5* has been reported to be a specific marker of peripheral arterial smooth muscle, is downregulated in atherosclerosis, and acts to inhibit SMC proliferation and neointimal formation,[47, 48] *Fn1* is a putative CAD GWAS gene thought to be protective in CAD and loss of function has been implicated in thoracic aortic aneurysm,[49, 50] and *Ccdc3* has been found to inhibit TNFα mediated vascular inflammation.[51]

Pathway analysis with genes which interact with differentially accessible chromatin regions from GREAT identifies key development pathways which characterize the ascending aorta such as 'heart development', 'heart morphogenesis', 'heart looping', while pathways which characterize the descending aorta include 'regionalization', 'anterior/posterior pattern specification', and 'embryonic organ development' demonstrating the residual chromatin accessibility of the embryonic developmental gene program (Supplemental Figure 1, panels A and B).

We then performed transcription factor motif accessibility analysis using ChromVAR as previously described.[35] In comparing ascending versus descending aorta SMCs, top differentially accessible motifs include numerous homeobox transcription factor motifs which have increased accessibility within SMCs from the descending aorta, including Cdx1 (caudal type homeobox 1), Lhx1 (LIM homeobox 1), Hoxd13, and Hoxc9 (Figure 2L&M). Other top motifs include Nrf1 (nuclear respiratory factor 1), and Znf281 (zinc finger protein 281). Importantly, two notable motifs with increased accessibility within the descending aorta include vascular protective transcription factors Klf15 (1.95 fold enrichment, *p=0.023*) and Yy1 (2.41 fold enrichment, *p=0.029*) (Figure 2N&O). *Klf15* has important roles in protecting against vascular inflammation while *Yy1* signaling inhibits SMC proliferation and intima formation.[52-55]

Fibroblast cell subset analysis reveals vascular bed specific gene programs and disease risk genes

Evaluation of fibroblasts subset population similarly reveals differences in chromatin accessibility and gene expression across vascular beds (Figure 1J). Differential peak accessibility analysis between fibroblasts from the ascending and descending aorta reveals 2,140 peaks which are differentially accessible. Top peaks which have higher accessibility in the ascending aorta include peaks located at chr9-24773927-24774846 and chr14-63271170-63272074 which lie 103bp and 87bp from the TSSs of *Tbx20* and *Gata4* respectively (Figure 3A-F). Peak to gene association analysis with GREAT reveals top genes with higher peak accessibility in the ascending aorta to include key developmental genes such as *Tbx20* and *Gata4* as well as signaling genes such as *Fam83a*, *Cul4b*, and *Cdkn2b* (Supplemental Table 5). Peaks with higher accessibility within the descending aorta include peaks which lie near the *Hoxa/b/c* family of transcription factors as well as other developmental transcription factors such as *Pax1* and *Foxd1* (Supplemental Table 5).

Gene ontology pathway analysis using GREAT software from differential chromatin peak accessibility identifies top pathways to be enriched in the ascending aorta to include developmental pathways such as ‘heart development’, ‘heart morphogenesis’, and ‘heart looping’, but also pathways which suggest a pro-calcification and extracellular matrix generation gene expression program with ‘regulation of ossification’, ‘bone development’, and ‘connective tissue development’ (Supplemental Figure 2, panel A). Pathways enriched within the descending aorta include ‘anterior/posterior pattern specification’ but also pathways which suggest a greater vascular development gene program including ‘angiogenesis’, ‘regulation of angiogenesis’, ‘regulation of vascular development’, ‘regulation of endothelial cell migration’, ‘Wnt signaling pathway’, and ‘branching morphogenesis of an epithelial tube’ (Supplemental Figure 2, panel B).

RNA expression analysis between vascular beds demonstrates significant concordance with peak accessibility analysis (Figure 3G). Fibroblast specific gene expression analysis reveals 436 genes which have differential expression between vascular beds (182 ascending,

127 carotid, 126 descending) (Supplemental Tables 6, 7, & 8). The top 10 genes which differentiate vascular beds include expected development genes such as *Tbx20*, *Hand2*, and *Hox* family transcription factors (Figure 3G). Interestingly, top 10 differentially expressed genes in the ascending aorta fibroblast population includes *Ptn* (pleiotrophin) an angiogenic growth factor involved in atherosclerosis,[56] *Wif1* (wnt inhibitory factor 1) a negative regulator of Wnt signaling which has been associated with coronary events,[57] and *Spon1* (spondin 1) an extracellular matrix gene which has been implicated in hypertension (Figure 3G, Supplemental Table 6).[58] Additional notable genes which have higher expression in the ascending aorta include CAD GWAS gene *Twist1* and osteogenic transcription factor *Sox9* (Figure 3H). Evaluation of genes which differentiate fibroblasts from the carotid vascular bed identifies several genes with associations with stroke including *Igfbp4* (insulin like growth factor binding protein 4) (Figure 3G&I, Supplemental Table 7), which has previously been found to be a plasma biomarker for ischemic stroke,[59] and *Sod3* (superoxide dismutase 3) (Figure 3G&J), for which polymorphisms have been implicated in the risk for ischemic stroke.[60] Top genes which differentiate fibroblasts in the descending aorta identify genes involved in TGFβ signaling such as *Tgfbi* (Figure 3G&K, Supplemental Table 8), cell adhesion molecules such as *Fbln7* (Figure 3G&L), and factors which regulate angiogenesis such as *Vegfd* and *Serpinf1* (Figure 3G).

Motif accessibility analysis using ChromVar between ascending and descending aorta fibroblasts reveals the SMAD2::SMAD3 motif as the top differentially accessible motif with higher accessibility within the ascending aorta (1.4 fold enrichment, P = 3.25E-40) (Figure 3M). *SMAD3* is a member of the TGFβ superfamily and has causal roles in aneurysm[61] and coronary artery disease.[62] Evaluation of the subsequent top differentially accessible motifs reveal the FOS and JUN family of transcription factors which have higher accessibility within the ascending aorta (Figure 3N). These factors include FOSL2, JUN, FOS::JUN, FOSL1::JUN, and FOS::JUND. FOS and JUN signaling within fibroblasts has been previously noted to promote

the development of a pro-fibrotic gene program,[63] has increased expression in human aneurysm,[64] and has been implicated in the development of atherosclerosis.[65]

Endothelial cell subset analysis shows distinct vascular bed specific VEGFR expression and ETS factor motif accessibility

Single cell analysis of endothelial cell subset population reveals vascular bed specific chromatin accessibility and gene expression programs (Figure 4). Visualization with UMAP demonstrates separation of endothelial cells from the ascending aorta with somewhat less pronounced differences between endothelial cells from the carotid artery and descending aorta (Figure 4A). Peak accessibility analysis between endothelial cells from the ascending and descending aorta identifies 223 peaks with differential accessibility meeting significance using an adjusted P value of 0.05. Top peaks which have increased accessibility in the ascending aorta includes peak chr6-134981222-134982145 which lies 34bp upstream of the TSS of *Apold1* (Figure 4B). Accessibility of this peak closely matches RNA expression of *Apold1* (Figure 4C). *Apold1* (apolipoprotein L domain containing 1, aka VERGE) has been previously reported as an endothelial cell specific stress response gene and protects against vascular thrombosis.[66, 67] Peak analysis similarly reveals that peak chr6-18031319-18032229, which lies 1189bp downstream of the TSS for *Wnt2*, has increased accessibility in the ascending aorta (Figure 4D) and this peak accessibility is strongly correlated with *Wnt2* expression (Figure 4E). Coverage plot of this genomic region demonstrates that chromatin accessibility is nearly entirely closed in the descending aorta with only minor accessibility in the carotid (Figure 4F). *Wnt2* has been shown to play important roles in endothelial-to-mesenchymal transition and the progression of atherosclerosis.[68] Notably, the descending aorta has increased accessibility of peak chr2-137109516-137110365 which lies 6703bp upstream of the TSS for *Jag1* (Figure 4G). Peak accessibility has a high correlation to *Jag1* gene expression (Figure 4H) and coverage plot of this genomic region reveals differential peak accessibility with carotid and descending

endothelial cells having similar accessibility (Figure 4I). *Jag1* (jagged 1) and associated Notch pathway signaling has important roles in suppressing vascular smooth muscle chondrogenic fate and in the formation of the atherosclerotic fibrous cap.[69, 70]

Differential gene expression analysis reveals specific patterns differentiating endothelial cell programs by vascular bed (Figure 4J) with FindMarker analysis identifying 273 differentially expressed genes between vascular beds (151 ascending, 6*2* carotid, 61 descending) (Supplemental Tables 9, 10, & 11). Ascending aortic endothelial cells have increased expression of VEGF receptors *Kdr* (kinase insert domain receptor, aka VEGFR), *Flt1* (fms related receptor tyrosine kinase 1, aka VEGFR1), and *Flt4* (fms related receptor tyrosine kinase 4, aka VEGFR3) (Supplemental Table 9). Carotid endothelial cells have higher expression of specific genes that appear to play unique roles within the cerebral vasculature. Top differentially expressed genes include *Efemp1* (EGF containing fibulin extracellular matrix protein 1) an extracellular matrix glycoprotein which regulates vessel development and has been associated with intracranial vascular disease and white matter density through large genome wide association studies,[71] and *Atp1b1* (ATPase Na+/K+ transporting subunit beta 1) which has been shown to have roles in mediating neuroprotection following cerebral ischemia (Supplemental Table 10).[72] Genes which are specific to endothelial cells isolated from the descending aorta include development genes such as *Nkx2-3* and Hox family genes such as *Hoxa7*, *Hoxb2*, and *Hoxb7* but also interestingly xenobiotic transformation gene *Cyp1b1* (cytochrome p450, 1b1) (Figure 4K). Vascular bed specific expression of *Cyp1b1* is particularly notable as it contributes to abdominal aortic aneurysm and suggests a vascular bed specific mechanism of aneurysm (Supplemental Table 11).[73, 74]

Motif accessibility analysis was performed comparing ascending and descending aortic endothelial cell populations. Top differentially accessible motifs reveal a significant increase in accessibility of multiple ETS factor motifs (E26 Transformation-specific Sequence) in the descending aorta (Figure 4L). ETS family members including ETV1 (1.74 fold enrichment),

ETV2 (2.0 fold), ETV4 (1.65 fold), ETS1 (1.92 fold), and EHF (1.65 fold) all have higher accessibility within the descending aorta (Figure 4L&M). ETS factors play important roles in cellular growth and differentiation and regulate vascular inflammation and remodeling where inhibition of ETS transcription factors promotes vessel regression.[75, 76]

Macrophage cells have minimal epigenomic and transcriptional variation across vascular beds

Given the significant vascular bed specific epigenomic and RNA transcriptional profiles observed within vascular SMCs, fibroblasts, and endothelial cells, we next evaluated if resident macrophages within healthy vascular tissues harbor specific epigenomic and transcriptional profiles. Macrophage cells from integrated scATACseq/scRNAseq data were subsetted and subsequently analyzed. Importantly, UMAP visualization of macrophage cells reveals no significant differences in macrophage cells across vascular beds (Figure 5A). Differential peak accessibility analysis between ascending and descending aorta macrophages do not reveal any peaks which meet statistical significance as differentially accessible. Differential gene expression analysis with scRNAseq data reveal very minimal differences in gene expression, with only 7 genes meeting statistical significance (4 in ascending, 1 carotid, 2 descending) (Figure 5B). This lack of vascular bed specific macrophage diversity across the aorta is notable given the contrasting finding within SMCs, fibroblasts, and endothelial cells, and that significant leukocyte diversity develops within the aorta during atherosclerosis.[77]

Epigenomic and transcriptional profiles of ascending and descending aortic tissue correspond to GWAS loci of aortic dimension

Data from these studies were employed to investigate vascular bed specific expression of genes which have recently been identified to influence ascending and descending aortic dimension.[17] Through an algorithm based method to evaluate cardiac MRI imaging of UK

Biobank participants, Pirrucello et al. (2022) identified 82 and 47 genomic loci which met genome wide significance for ascending and descending aortic dimensions, respectively. By taking the nearest gene for each locus, we generated an ascending and descending aortic dimension score for each individual cell based on the expression of each gene.

We identified that for both the ascending and descending aortic scores, SMCs have the highest score when compared to fibroblasts, endothelial cells, or macrophage cells (Figure 6A-F). Interestingly, the ascending and descending aorta scores within SMCs reveal no difference between vascular beds (Figure 6B&E). However, we observed that the ascending and descending aorta scores within fibroblasts are notably higher within fibroblasts isolated from the ascending aorta, highlighting vascular bed specific aortic dimension scores and suggesting that genetic mechanisms of aortic dimension may be particularly relevant within vascular fibroblasts (Figure 6C&F). Evaluation of the genes which drive the ascending aorta GWAS score within fibroblasts reveal *Wwp2*, *Fbn1*, *Ncam1*, *Jmjd1c*, *Fbxo32*, *Angpt1*, *Tbx20*, *Hand2*, *Col6a3*, and *Zeb2* as being differentially expressed between vascular beds (Figure 6G). Genes which modify the descending aorta dimension score include overlapping genes such as *Tbx20* and *Wwp2* but also descending aorta specific genes such as *Fhl1*, *Lmcd1*, and *Nav1* (Figure 6H). *Hand2* has higher expression within the fibroblasts isolated from the ascending aorta and carotid artery compared to the descending aorta and the coverage plot reveals increased chromatin accessibility of enhancers within the ascending and carotid fibroblasts (Figure 6I). *Col6a3* has higher expression within the descending aorta and coverage plot shows a consistent finding of higher peak accessibility within fibroblasts of the descending aorta (Figure 6J). *Wwp2* has higher expression in fibroblasts of the ascending aorta (Figure 6K) and the coverage plot shows higher peak accessibility of specific enhancers (Figure 6L). *Wwp2* (WW domain-containing E3 ubiquitin protein ligase 2) is a ubiquitin ligase that promotes the degradation of the tumor suppressor PTEN,[78] raising the possible unique role of PTEN signaling in fibroblast function and vascular dimension.

This work thus reveals that epigenetic enhancers of vascular cells are vascular bed specific and appear weighted towards disease risk genes. These findings suggest unique vascular bed specific disease mechanisms driven by vascular bed specific epigenomic landscapes.

Primary adventitial fibroblast response to TGFβ is dependent on vascular bed and implicates functional developmental epigenomic memory

We have shown that vascular SMCs, fibroblasts, and endothelial cells have transcriptional and epigenomic features that are distinct to vascular bed. Further, TF motif accessibility analysis in fibroblasts reveals an increased accessibility of SMAD2:SMAD3, FOS, and JUN motifs in the ascending fibroblast population compared to carotid and descending fibroblasts (Fig 3M&N). This differential chromatin accessibility would suggest the potential for heightened biological response to TGFβ in ascending fibroblasts. To evaluate the functional effect of this differential chromatin accessibility and to identify if differential gene expression is retained following removal from vascular bed flow conditions, we isolated and cultured primary adventitial fibroblasts from healthy 14 week old C57BL/6 mice from the ascending and descending aorta and stimulated them with control or TGFβ (10ng/mL, 48hrs) and performed bulk RNA sequencing (n = 3 per condition) (Fig 7A).

Principal component analysis (PCA) of RNAseq data reveals distinct separation of samples based on origin of vascular bed and stimulation with TGFβ (Fig 7B). Upon evaluation of differential gene expression by site of vascular bed, we observe 1342 differentially expressed genes between ascending and descending fibroblasts (Fig 7C). Ascending fibroblasts have increased expression of genes including *Hand2*, *Tbx20*,

Pcolce2, *Tcf21*, and *Gata4* (Fig 7C, Supplemental Fig 3, Supplemental Table 12), while descending fibroblasts have increased expression of *Hox* family of genes (i.e. *Hoxb9*, *Hoxa7*, *Hoxc8*), *Col6a3*, and *Pax1* (Fig 7C, Supplemental Fig 3, Supplemental Table 13). When evaluating response to TGFβ stimulation, comparing all samples by TGFβ treatment, we identify 4,234 DE genes, with top upregulated genes including *Ada*, *Snx30*, *Wisp1*, *Cthrc1*, *Loxl2*, and *Akap5*, (Fig 7D, Supplemental Table 14) while top downregulated genes include *Adm*, *Gstm1*, *Mcc*, *Rras2*, *Il6ra*, and *Vegfd* (Fig 7D, Supplemental Table 15). To evaluate the effect of TGFβ by vascular bed, we compared the transcriptomic effect of TGFβ stimulation within ascending and descending fibroblast samples. We identify TGFβ stimulation to induce a markedly higher transcriptional effect in ascending fibroblasts, with 6,733 DE genes (Fig 7E, Supplemental Tables 16 and 17) while only 2,250 DE genes within descending fibroblasts (Fig 7F, Supplemental Tables 18 and 19).

By performing an interaction analysis — which evaluates the differential log2FoldChange of TGFβ treatment by vessel type — we identify 422 genes that meet FDR cutoff for interaction significance (Supplemental Fig 4, Supplemental Table 20). We identify that matrix gene *Eln* has much lower expression in descending fibroblasts but is rapidly upregulated in response to TGFβ (Supplemental Fig 4). Interaction analysis reveals key genes with differential response to TGFβ by vascular bed, including TGFβ response genes *Meox1* and *Gdf6* that are more highly induced in ascending fibroblasts, while *Tgfb1* and *Tgfb3* are more induced in descending fibroblasts, suggesting an enhanced regulatory feedback in ascending fibroblasts (Supplemental Fig 4, Supplemental Table 20). Numerous collagen genes have

differential response to TGFβ by vascular bed, where *Col8a1* and *Col5a2* are upregulated by TGFβ to a greater extent in descending fibroblasts (Supplemental Fig 4). Alternatively, *Col28a1* and *Col6a1* are downregulated by TGFβ to a greater extent in descending fibroblasts (Supplemental Fig 4). TFs such as *Klf4* and *Ptx3* are more highly expressed in ascending fibroblasts and then downregulated by TGFβ to a greater extent than descending fibroblasts (Supplemental Fig 4). However, *Ahr* is downregulated by TGFβ in descending fibroblasts only while *Hoxb5* shows differing effects by vascular bed, where it is modestly upregulated in ascending while downregulated in descending fibroblasts (Supplemental Fig 4).

By evaluating the 200bp DNA sequence upstream of the transcription start site of differentially expressed RNA transcripts, we evaluated TF motif enrichment using HOMER. In control samples, DE genes upregulated in ascending vs descending fibroblasts reveal enrichment of key TFs including SMAD3 (TWGTCTGV), KLFs including KLF4 (GCCACACCCA), FOS (NDATGASTCAYN), and HIF1α (TACGTGCV)(p-values 1.0E-10, 1.0E-13, 1.0E-07, and 1.0E-05, respectively). DE genes upregulated in descending fibroblasts reveal enrichment of TFs including HOXA11 (TTTTATGGCM), HOXA9 (RGCAATNAAA), HOXC6 (GGCCATAAATCA), (p-values 1.0E-07, 1.0E-06, 1.0E-03, respectively) (Fig 7G&H). Enrichment of these TFs in differentially expressed genes indicate that these motifs with increased chromatin accessibility have significant functional effect on global transcriptome.

Vascular bed specific Meox1 activation implicates epigenetic 'priming' for fibroblast activation in ascending aortic fibroblasts

Our findings implicate a cell type and vascular bed specific ‘epigenetic memory’ of important regulatory enhancer elements with functional effect on disease relevant pathways. A notable observation is that in primary adventitial fibroblasts, *Meox1* expression is upregulated to a much greater extent in response to TGFβ compared to descending fibroblasts (Supplemental Fig 4C). *Meox1* has recently been described as a master regulator of fibroblast activation in cardiac fibroblasts through epigenetic mechanisms.[20] Although we observed *Meox1* to be upregulated in response to TGFβ to a greater extent in ascending fibroblasts, baseline expression appeared similar, or less than, descending fibroblasts (Supplemental Fig 4). To investigate if there is differential RNA expression and chromatin accessibility in fibroblasts *in vivo*, we interrogated our scRNAseq and scATACseq fibroblast dataset. We see that *Meox1* has increased RNA expression in ascending fibroblasts, but this expression is largely limited to a specific cell population that represents valvular fibroblasts (Supplemental Fig 5A&B). Importantly, when investigating for *Meox1* chromatin accessibility, we see that *Meox1* chromatin accessibility is much more expansive and extends throughout all ascending fibroblasts, with increased total chromatin accessibility in the ascending fibroblasts (Supplemental Fig 5C&D). This discrepancy of chromatin accessibility and RNA expression for non-valvular ascending fibroblasts gives strong evidence to support an epigenetic ‘priming’, where following activation with TGFβ, *Meox1* is rapidly upregulated in ascending compared to descending fibroblasts.

Discussion

Chromatin architecture and cis-regulatory elements such as enhancers and promoters are critical in mediating cellular gene programs in a cell type specific manner.[19] Disease associated gene variants identified through GWAS are now increasingly being recognized to influence disease risk through modification of these regulatory regions of the genome.[79] Additionally, there is now growing experimental evidence that vascular disease associated gene loci influence disease risk in cell type specific mechanisms, where common human genetic variation can modify the function of cell type specific enhancers.[22, 23] Risk of vascular diseases, such as atherosclerosis, aneurysm, or autoinflammatory vasculitides, are vascular bed specific, with disease associated genetic loci suggesting differing genetic mechanisms of disease. These observations raise the question as to what extent do cell type specific enhancers and gene programs vary by vascular bed, and do these variations contribute to disease risk?

Through use of single cell epigenomic and transcriptomic profiling with scATACseq and scRNAseq, we evaluated cell type and vascular bed specific enhancer and gene expression profiles of healthy vascular tissue in adult mice from three disease relevant vascular beds, 1) ascending aorta and aortic root, 2) brachiocephalic and right common carotid arteries, and 3) descending thoracic aorta (Figure 1A). These vascular beds represent the developmental diversity which makes up the aorta, with these regions arising from the secondary heart field and neural crest, neural crest, and somitic mesoderm, respectively. This work has revealed thousands of differentially accessible enhancers within vascular smooth muscle, fibroblasts, and endothelial cells, across these three vascular beds. Similarly, differential chromatin accessibility was found to correspond to hundreds of differentially expressed genes within cell type between

vascular beds. Strikingly, there were no differences observed in resident macrophages between vascular beds, an observation which highlights that this phenomenon is specific to cells of the vascular wall and reflect developmental origin.

The activation of key developmental transcription factors is crucial in the coordinated cellular development of the fetal and adult vasculature. Although expression of genes such as *Hand2*, *Tbx20*, *Gata4*, *Wnt* and those encoding related WNT signaling molecules, and *Hoxa/b/c* family of transcription factors have previously been known to mediate vascular development,[5, 8, 25-28] the residual chromatin accessibility and gene expression of these developmental transcription factors in the adult vasculature has been less well characterized. A notable observation of our study is that key regulatory enhancers of development genes *Tbx20*, *Hand2*, and *Gata4* have increased chromatin accessibility in the ascending aorta and carotid artery in comparison to the descending aorta in smooth muscle and fibroblasts, and to a lesser extent in endothelial cells (Figures 2&3). Whereas *Hoxb* and *Hoxa/Hoxc* family of transcription factors have increased chromatin accessibility in the descending aorta (Figures 2&3). These findings highlight that these vascular cells retain an epigenetic 'memory' of their developmental program, suggesting these cells are poised to turn on these gene programs.

This finding further raises the question as to the role of these development genes in mediating vascular disease risk in adulthood. Although genetic variation in *TBX20* has been associated with a spectrum of congenital cardiac lesions relating to cardiac and vascular development,[80] there have been increasing observations that genetic loci near *TBX20* meet genome wide significance for disease in adulthood including coronary

artery disease,[81] myocardial infarction,[82] blood pressure,[83] and aortic dimension and distensibility.[17, 84] Similarly, variants near *GATA4* and members of the *HOXB* family of transcription factors such as *HOXB7* have been associated with hypertension,[85, 86] while *HAND2* variants are associated with aortic dimension and atrial fibrillation.[17, 87] The vascular bed and cell type specific chromatin accessibility observed in our study of these developmental transcription factors may suggest their ongoing role in mediating vascular disease in adulthood in a vascular bed specific mechanism. This hypothesis of developmental TFs involved in vascular disease pathogenesis has been similarly supported by work from our lab on developmental TFs *TCF21* and *ZEB2.*[22, 31] These TFs — which have important roles in vascular development, regulating cell state transitions and endothelial to mesenchymal transition[88, 89] — have been identified through GWAS as having additional roles in the development of CAD.[12, 44] SMC specific deletion of *Tcf21* and *Zeb2* in the mouse revealed a significant effect on transcriptional regulation, epigenetic landscape, and plaque characteristic, further defining their roles as causal CAD genes.[22, 31]

TF motif accessibility analysis identified an important observation that SMAD2:SMAD3 motif is enriched in ascending aortic fibroblasts, highlighting a potential vascular bed specific response to TGFβ signaling. By isolating and culturing primary adventitial fibroblasts from ascending and descending aorta, *in vitro* experiments with TGFβ stimulation with bulk RNA sequencing confirmed that differential gene expression by vascular bed is retained following isolation and *in vitro* culture and revealed ascending fibroblasts to have a markedly greater response to TGFβ than descending fibroblasts (Fig 7). These are two important observations that reveals 1) DE genes by

vascular bed in fibroblasts are independent of differential laminar and turbulent flow and 2) implicates differential chromatin accessibility and relevant TF motif accessibility to have causal biological and disease relevant function. Evaluation of the master regulator of fibroblast activation *Meox1*[20] further identifies an epigenetic 'priming' of key disease relevant genes. Primary fibroblast culture shows similar baseline RNA expression of *Meox1* between vascular beds, but *Meox1* is upregulated to a much greater extent in ascending fibroblasts in response to TGFβ (Supplemental Fig 4C). This differential effect is likely driven by increased chromatin accessibility, where *in vivo Meox1* chromatin accessibility is increased in ascending fibroblasts with discordant minimal RNA expression (Supplemental Fig 5), suggesting an accessible chromatin landscape of *Meox1* that is more favorable to activation.

Importantly, differential chromatin accessibility and gene expression profiles between vascular beds highlight specific genes with known roles in mediating vascular disease. For example, expression of the gene *Ccn3* is higher in the ascending aorta smooth muscle (Figure 2I). Prior experimental work has shown that *Ccn3* inhibits neointima formation through inhibition of vascular smooth muscle proliferation and regulation of macrophage foam cell formation, while overexpression of *Ccn3* inhibits vascular inflammation and is protective against atherosclerosis in mice.[40, 41, 90] Given the differential expression of *Ccn3* between vascular beds, one hypothesis may be that this *Ccn3* pathway plays differing roles in mediating disease across vascular beds. Perhaps this suggests that augmenting this pathway may prove to have a greater benefit in vascular beds which are 'deficient' in *Ccn3*, i.e. carotid artery and descending thoracic aorta. An alternative hypothesis may be that this pathway has particular importance

within the ascending aorta and that increasing *Ccn3* signaling may have greatest benefit within this vascular bed or that the ascending aorta is particularly sensitive to loss of *Ccn3* signaling. Similar hypotheses could be made for genes such as *Tns1* which has higher expression in the ascending aorta SMCs, *Junb* and *Atf3* which have higher expression within the carotid artery SMCs, as well as *Rgs5* and *Fn1* which have higher expression within the descending aorta SMCs, each of which have significant evidence behind their roles in mediating vascular disease.[23, 44, 45, 47-50]

A finding which further supports the hypothesis that differentially expressed genes play specific roles in vascular bed specific disease risk is that differentially expressed genes appear to have notable roles in vascular bed specific diseases such as risk of stroke in the carotid artery and risk of abdominal aortic aneurysm in the descending thoracic aorta. This observation was noted for *Igfbp4* and *Sod3* which have higher expression within fibroblasts isolated from the carotid artery, both of which have been implicated in risk of stroke.[59, 60] A particularly notable finding consistent with differential gene expression matching vascular bed specific disease risk is that *Cyp1b1* has higher expression within the descending aorta endothelial cell population (Figure 3K). *Cyp1b1* has a particularly important role in mediating the formation of abdominal aortic aneurysm in mice.[73, 74] Our observation that *Cyp1b1* has higher expression and greater chromatin accessibility within the endothelium of the descending aorta and that this gene plays particular importance in the development of aneurysm within this vascular bed suggests this gene to have a selective role in mediating vascular bed specific disease risk. This is a particularly interesting observation as exposure to cigarette smoke carries a high risk for developing abdominal aortic aneurysm and

cigarette smoke itself is a strong inducer of *Cyp1b1*, calling into question the potential '*Gene X Environment*' interaction in mediating risk of abdominal aortic aneurysm.[91, 92]

Limitations

In this study, our aim was to evaluate single cell enhancer and transcriptional profiles across vascular beds in healthy tissue. A limitation of this study is that we did not evaluate the epigenomic profiles in a disease state across vascular beds. However, by isolating and culturing primary adventitial fibroblasts and evaluating differential response to TGFβ, we gained further insight into this mechanism. We anticipate that there are dynamic changes in chromatin accessibility and gene expression programs in disease, as has been previously observed,[22, 23] and future studies will be aimed at understanding how these dynamic chromatin accessibility changes occur across vascular beds. Similarly, recent work has demonstrated changes in chromatin accessibility in vascular tissue with aging.[93] Our study selected for adult mice that are 14-16 weeks of age, which represents a young adult. We anticipate that chromatin accessibility dynamically changes with aging and future studies to evaluate how this change differs across vascular beds may be particularly insightful.

Conclusions

By performing combined scRNAseq and scATACseq on vascular tissue across three vascular beds, we reveal for the first time that the epigenomic landscape and transcriptional profiles of vascular smooth muscle, fibroblasts, and endothelial cells, are specific to anatomic origin. Further, isolation and culturing of primary adventitial

fibroblasts from ascending and descending aorta emphasized that this differential gene response is retained following *in vitro* culture and modifies response to TGFβ. The genomic regions and genes that differentiate cells by vascular bed are strongly weighted towards developmental genes, demonstrating that vascular cells have an epigenetic 'memory' of their developmental program. In addition, differential chromatin accessibility appears to 'prime' vascular bed specific gene regulatory networks in disease relevant mechanisms. Beyond development genes, differentially accessible regions across vascular beds are heavily weighted towards genes with known roles in mediating vascular disease risk, providing unique insight into the potential for vascular bed specific disease mechanisms. This work supports the hypothesis that the epigenomic landscape of vascular cells are not only cell type specific, but vascular bed specific and influence vascular bed specific disease risk. This provides a paradigm that genetic mechanisms of disease influences risk in a vascular bed specific manner, gives unique insight into vascular bed specific transcriptional and epigenetic programs, and further creates a valuable single cell atlas for the vascular biology community.

Acknowledgements

This work was supported by National Institutes of Health grants F32HL160067 (CW), L30HL159413 (CW), K08HL153798 (PC), F32HL154681 (AJP), F32HL160058 (ARD), R01HL157949 (MPF), R01HL134817 (TQ), R01HL139478 (TQ), R01HL156846 (TQ), R01HL151535 (TQ), R01HL145708 (TQ), UM1 HG011972 (TQ), as well as a Human Cell Atlas grant from the Chan Zuckerberg Foundation. This work was also supported

by American Heart Association grant 20CDA35310303 (PC), 23CDA1042900 (CW), and 23POST1018991 (WG).

Disclosures

TQ is a scientific advisor for Amgen. CSW has consulted for Tensixteen Bio and Renovacor. All other authors have no disclosures.

References

1. Haimovici H and Maier N. Fate of Aortic Homografts in Canine Atherosclerosis. 3. Study of Fresh Abdominal and Thoracic Aortic Implants into Thoracic Aorta: Role of Tissue Susceptibility in Atherogenesis. *Arch Surg*. 1964;89:961-9.
2. Haimovici H, Maier N and Strauss L. Fate of aortic homografts in experimental canine atherosclerosis; study of fresh thoracic implants into abdominal aorta. *AMA Arch Surg*. 1958;76:282-8.
3. Haimovici H, Maier N and Strauss L. Fate of aortic homografts in experimental canine atherosclerosis. II. Study of fresh abdominal aortic implants into abdominal aorta. *AMA Arch Surg*. 1959;78:239-45.
4. Katz TC, Singh MK, Degenhardt K, Rivera-Feliciano J, Johnson RL, Epstein JA and Tabin CJ. Distinct compartments of the proepicardial organ give rise to coronary vascular endothelial cells. *Dev Cell*. 2012;22:639-50.
5. Majesky MW. Developmental basis of vascular smooth muscle diversity. *Arterioscler Thromb Vasc Biol*. 2007;27:1248-58.
6. Mikawa T and Gourdie RG. Pericardial mesoderm generates a population of coronary smooth muscle cells migrating into the heart along with ingrowth of the epicardial organ. *Dev Biol*. 1996;174:221-32.
7. Red-Horse K, Ueno H, Weissman IL and Krasnow MA. Coronary arteries form by developmental reprogramming of venous cells. *Nature*. 2010;464:549-53.
8. Sawada H, Rateri DL, Moorleghen JJ, Majesky MW and Daugherty A. Smooth Muscle Cells Derived From Second Heart Field and Cardiac Neural Crest Reside in Spatially Distinct Domains in the Media of the Ascending Aorta-Brief Report. *Arterioscler Thromb Vasc Biol*. 2017;37:1722-1726.
9. Tian X, Hu T, Zhang H, He L, Huang X, Liu Q, Yu W, He L, Yang Z, Zhang Z, Zhong TP, Yang X, Yang Z, Yan Y, Baldini A, Sun Y, Lu J, Schwartz RJ, Evans SM, Gittenberger-de Groot AC, Red-Horse K and Zhou B. Subepicardial endothelial cells invade the embryonic ventricle wall to form coronary arteries. *Cell Res*. 2013;23:1075-90.

10. Volz KS, Jacobs AH, Chen HI, Poduri A, McKay AS, Riordan DP, Kofler N, Kitajewski J, Weissman I and Red-Horse K. Pericytes are progenitors for coronary artery smooth muscle. *Elife*. 2015;4.
11. Jones GT, Tromp G, Kuivaniemi H, Gretarsdottir S, Baas AF, Giusti B, Strauss E, Van't Hof FN, Webb TR, Erdman R, Ritchie MD, Elmore JR, Verma A, Pendergrass S, Kullo IJ, Ye Z, Peissig PL, Gottesman O, Verma SS, Malinowski J, Rasmussen-Torvik LJ, Borthwick KM, Smelser DT, Crosslin DR, de Andrade M, Ryer EJ, McCarty CA, Bottinger EP, Pacheco JA, Crawford DC, Carrell DS, Gerhard GS, Franklin DP, Carey DJ, Phillips VL, Williams MJ, Wei W, Blair R, Hill AA, Vasudevan TM, Lewis DR, Thomson IA, Krysa J, Hill GB, Roake J, Merriman TR, Oszkinis G, Galora S, Saracini C, Abbate R, Pulli R, Pratesi C, Saratzis A, Verissimo AR, Bumpstead S, Badger SA, Clough RE, Cockerill G, Hafez H, Scott DJ, Futers TS, Romaine SP, Bridge K, Griffin KJ, Bailey MA, Smith A, Thompson MM, van Bockxmeer FM, Matthiasson SE, Thorleifsson G, Thorsteinsdottir U, Blankensteijn JD, Teijink JA, Wijmenga C, de Graaf J, Kiemeney LA, Lindholt JS, Hughes A, Bradley DT, Stirrups K, Golledge J, Norman PE, Powell JT, Humphries SE, Hamby SE, Goodall AH, Nelson CP, Sakalihasan N, Courtois A, Ferrell RE, Eriksson P, Folkersen L, Franco-Cereceda A, Eicher JD, Johnson AD, Betsholtz C, Ruusalepp A, Franzen O, Schadt EE, Bjorkegren JL, Lipovich L, Drolet AM, Verhoeven EL, Zeebregts CJ, Geelkerken RH, van Sambeek MR, van Sterkenburg SM, de Vries JP, Stefansson K, Thompson JR, de Bakker PI, Deloukas P, Sayers RD, Harrison SC, van Rij AM, Samani NJ and Bown MJ. Meta-Analysis of Genome-Wide Association Studies for Abdominal Aortic Aneurysm Identifies Four New Disease-Specific Risk Loci. *Circ Res*. 2017;120:341-353.
12. Nikpay M, Goel A, Won HH, Hall LM, Willenborg C, Kanoni S, Saleheen D, Kyriakou T, Nelson CP, Hopewell JC, Webb TR, Zeng L, Dehghan A, Alver M, Armasu SM, Auro K, Bjonnes A, Chasman DI, Chen S, Ford I, Franceschini N, Gieger C, Grace C, Gustafsson S, Huang J, Hwang SJ, Kim YK, Kleber ME, Lau KW, Lu X, Lu Y, Lyytikainen LP, Mihailov E, Morrison AC, Pervjakova N, Qu L, Rose LM, Salfati E, Saxena R, Scholz M, Smith AV, Tikkanen E, Uitterlinden A, Yang X, Zhang W, Zhao W, de Andrade M, de Vries PS, van Zuydam NR, Anand SS, Bertram L, Beutner F, Dedoussis G, Frossard P, Gauguier D, Goodall AH, Gottesman O, Haber M, Han BG, Huang J, Jalilzadeh S, Kessler T, Konig IR, Lannfelt L, Lieb W, Lind L, Lindgren CM, Lokki ML, Magnusson PK, Mallick NH, Mehra N, Meitinger T, Memon FU, Morris AP, Nieminen MS, Pedersen NL, Peters A, Rallidis LS, Rasheed A, Samuel M, Shah SH, Sinisalo J, Stirrups KE, Trompet S, Wang L, Zaman KS, Ardissino D, Boerwinkle E, Borecki IB, Bottinger EP, Buring JE, Chambers JC, Collins R, Cupples LA, Danesh J, Demuth I, Elosua R, Epstein SE, Esko T, Feitosa MF, Franco OH, Franzosi MG, Granger CB, Gu D, Gudnason V, Hall AS, Hamsten A, Harris TB, Hazen SL, Hengstenberg C, Hofman A, Ingelsson E, Iribarren C, Jukema JW, Karhunen PJ, Kim BJ, Kooner JS, Kullo IJ, Lehtimaki T, Loos RJF, Melander O, Metspalu A, Marz W, Palmer CN, Perola M, Quertermous T, Rader DJ, Ridker PM, Ripatti S, Roberts R, Salomaa V, Sanghera DK, Schwartz SM, Seedorf U, Stewart AF, Stott DJ, Thiery J, Zalloua PA, O'Donnell CJ, Reilly MP, Assimes TL, Thompson JR, Erdmann J, Clarke R, Watkins H, Kathiresan S, McPherson R, Deloukas P, Schunkert H, Samani NJ and Farrall M. A comprehensive 1,000 Genomes-based genome-wide association meta-analysis of coronary artery disease. *Nat Genet*. 2015;47:1121-1130.

13. Schunkert H, Konig IR, Kathiresan S, Reilly MP, Assimes TL, Holm H, Preuss M, Stewart AF, Barbalic M, Gieger C, Absher D, Aherrahrou Z, Allayee H, Altshuler D, Anand SS, Andersen K, Anderson JL, Ardissino D, Ball SG, Balmforth AJ, Barnes TA, Becker DM, Becker LC, Berger K, Bis JC, Boekholdt SM, Boerwinkle E, Braund PS, Brown MJ, Burnett MS, Buysschaert I, Cardiogenics, Carlquist JF, Chen L, Cichon S, Codd V, Davies RW, Dedoussis G, Dehghan A, Demissie S, Devaney JM, Diemert P, Do R, Doering A, Eifert S, Mokhtari NE, Ellis SG, Elosua R, Engert JC, Epstein SE, de Faire U, Fischer M, Folsom AR, Freyer J, Gigante B, Girelli D, Gretarsdottir S, Gudnason V, Gulcher JR, Halperin E, Hammond N, Hazen SL, Hofman A, Horne BD, Illig T, Iribarren C, Jones GT, Jukema JW, Kaiser MA, Kaplan LM, Kastelein JJ, Khaw KT, Knowles JW, Kolovou G, Kong A, Laaksonen R, Lambrechts D, Leander K, Lettre G, Li M, Lieb W, Loley C, Lotery AJ, Mannucci PM, Maouche S, Martinelli N, McKeown PP, Meisinger C, Meitinger T, Melander O, Merlini PA, Mooser V, Morgan T, Muhleisen TW, Muhlestein JB, Munzel T, Musunuru K, Nahrstaedt J, Nelson CP, Nothen MM, Olivieri O, Patel RS, Patterson CC, Peters A, Peyvandi F, Qu L, Quyyumi AA, Rader DJ, Rallidis LS, Rice C, Rosendaal FR, Rubin D, Salomaa V, Sampietro ML, Sandhu MS, Schadt E, Schafer A, Schillert A, Schreiber S, Schrezenmeir J, Schwartz SM, Siscovick DS, Sivananthan M, Sivapalaratnam S, Smith A, Smith TB, Snoep JD, Soranzo N, Spertus JA, Stark K, Stirrups K, Stoll M, Tang WH, Tennstedt S, Thorgeirsson G, Thorleifsson G, Tomaszewski M, Uitterlinden AG, van Rij AM, Voight BF, Wareham NJ, Wells GA, Wichmann HE, Wild PS, Willenborg C, Witteman JC, Wright BJ, Ye S, Zeller T, Ziegler A, Cambien F, Goodall AH, Cupples LA, Quertermous T, Marz W, Hengstenberg C, Blankenberg S, Ouwehand WH, Hall AS, Deloukas P, Thompson JR, Stefansson K, Roberts R, Thorsteinsdottir U, O'Donnell CJ, McPherson R, Erdmann J, Consortium CA and Samani NJ. Large-scale association analysis identifies 13 new susceptibility loci for coronary artery disease. *Nat Genet*. 2011;43:333-8.
14. van der Harst P and Verweij N. Identification of 64 Novel Genetic Loci Provides an Expanded View on the Genetic Architecture of Coronary Artery Disease. *Circ Res*. 2018;122:433-443.
15. Strawbridge RJ, Ward J, Bailey MES, Cullen B, Ferguson A, Graham N, Johnston KJA, Lyall LM, Pearsall R, Pell J, Shaw RJ, Tank R, Lyall DM and Smith DJ. Carotid Intima-Media Thickness: Novel Loci, Sex-Specific Effects, and Genetic Correlations With Obesity and Glucometabolic Traits in UK Biobank. *Arterioscler Thromb Vasc Biol*. 2020;40:446-461.
16. Franceschini N, Giambartolomei C, de Vries PS, Finan C, Bis JC, Huntley RP, Lovering RC, Tajuddin SM, Winkler TW, Graff M, Kavousi M, Dale C, Smith AV, Hofer E, van Leeuwen EM, Nolte IM, Lu L, Scholz M, Sargurupremraj M, Pitkanen N, Franzen O, Joshi PK, Noordam R, Marioni RE, Hwang SJ, Musani SK, Schminke U, Palmas W, Isaacs A, Correa A, Zonderman AB, Hofman A, Teumer A, Cox AJ, Uitterlinden AG, Wong A, Smit AJ, Newman AB, Britton A, Ruusalepp A, Sennblad B, Hedblad B, Pasaniuc B, Penninx BW, Langefeld CD, Wassel CL, Tzourio C, Fava C, Baldassarre D, O'Leary DH, Teupser D, Kuh D, Tremoli E, Mannarino E, Grossi E, Boerwinkle E, Schadt EE, Ingelsson E, Veglia F, Rivadeneira F, Beutner F, Chauhan G, Heiss G, Snieder H, Campbell H, Volzke H, Markus HS, Deary IJ, Jukema JW, de Graaf J, Price J, Pott J, Hopewell JC, Liang J, Thiery J, Engmann J, Gertow K, Rice K, Taylor KD,

Dhana K, Kiemeney L, Lind L, Raffield LM, Launer LJ, Holdt LM, Dorr M, Dichgans M, Traylor M, Sitzer M, Kumari M, Kivimaki M, Nalls MA, Melander O, Raitakari O, Franco OH, Rueda-Ochoa OL, Roussos P, Whincup PH, Amouyel P, Giral P, Anugu P, Wong Q, Malik R, Rauramaa R, Burkhardt R, Hardy R, Schmidt R, de Mutsert R, Morris RW, Strawbridge RJ, Wannamethee SG, Hagg S, Shah S, McLachlan S, Trompet S, Seshadri S, Kurl S, Heckbert SR, Ring S, Harris TB, Lehtimaki T, Galesloot TE, Shah T, de Faire U, Plagnol V, Rosamond WD, Post W, Zhu X, Zhang X, Guo X, Saba Y, Consortium M, Dehghan A, Seldenrijk A, Morrison AC, Hamsten A, Psaty BM, van Duijn CM, Lawlor DA, Mook-Kanamori DO, Bowden DW, Schmidt H, Wilson JF, Wilson JG, Rotter JI, Wardlaw JM, Deanfield J, Halcox J, Lyytikainen LP, Loeffler M, Evans MK, Debette S, Humphries SE, Volker U, Gudnason V, Hingorani AD, Bjorkegren JLM, Casas JP and O'Donnell CJ. GWAS and colocalization analyses implicate carotid intima-media thickness and carotid plaque loci in cardiovascular outcomes. *Nat Commun*. 2018;9:5141.

17. Pirruccello JP, Chaffin MD, Chou EL, Fleming SJ, Lin H, Nekoui M, Khurshid S, Friedman SF, Bick AG, Arduini A, Weng LC, Choi SH, Akkad AD, Batra P, Tucker NR, Hall AW, Roselli C, Benjamin EJ, Vellarikkal SK, Gupta RM, Stegmann CM, Juric D, Stone JR, Vasan RS, Ho JE, Hoffmann U, Lubitz SA, Philippakis AA, Lindsay ME and Ellinor PT. Deep learning enables genetic analysis of the human thoracic aorta. *Nat Genet*. 2022;54:40-51.

18. Oudelaar AM and Higgs DR. The relationship between genome structure and function. *Nat Rev Genet*. 2021;22:154-168.

19. Anene-Nzelu CG, Lee MCJ, Tan WLW, Dashi A and Foo RSY. Genomic enhancers in cardiac development and disease. *Nat Rev Cardiol*. 2022;19:7-25.

20. Alexanian M, Przytycki PF, Micheletti R, Padmanabhan A, Ye L, Travers JG, Gonzalez-Teran B, Silva AC, Duan Q, Ranade SS, Felix F, Linares-Saldana R, Li L, Lee CY, Sadagopan N, Pelonero A, Huang Y, Andreoletti G, Jain R, McKinsey TA, Rosenfeld MG, Gifford CA, Pollard KS, Haldar SM and Srivastava D. A transcriptional switch governs fibroblast activation in heart disease. *Nature*. 2021;595:438-443.

21. Hocker JD, Poirion OB, Zhu F, Buchanan J, Zhang K, Chiou J, Wang TM, Zhang Q, Hou X, Li YE, Zhang Y, Farah EN, Wang A, McCulloch AD, Gaulton KJ, Ren B, Chi NC and Preissl S. Cardiac cell type-specific gene regulatory programs and disease risk association. *Sci Adv*. 2021;7.

22. Cheng P, Wirka RC, Clarke LS, Zhao Q, Kundu R, Nguyen T, Nair S, Sharma D, Kim HJ, Shi H, Assimes T, Kim JB, Kundaje A and Quertermous T. ZEB2 Shapes the Epigenetic Landscape of Atherosclerosis. *Circulation*. 2022.

23. Wang Y, Gao H, Wang F, Ye Z, Mokry M, Turner AW, Ye J, Koplev S, Luo L, Alsaigh T, Adkar SS, Elishaev M, Gao X, Maegdefessel L, Bjorkegren JLM, Pasterkamp G, Miller CL, Ross EG and Leeper NJ. Dynamic changes in chromatin accessibility are associated with the atherogenic transitioning of vascular smooth muscle cells. *Cardiovasc Res*. 2021.

24. Depuydt MAC, Prange KHM, Slenders L, Ord T, Elbersen D, Boltjes A, de Jager SCA, Asselbergs FW, de Borst GJ, Aavik E, Lonnberg T, Lutgens E, Glass CK, den Ruijter HM, Kaikkonen MU, Bot I, Slutter B, van der Laan SW, Yla-Herttuala S, Mokry M, Kuiper J, de Winther MPJ and Pasterkamp G. Microanatomy of the Human Atherosclerotic Plaque by Single-Cell Transcriptomics. *Circ Res*. 2020;127:1437-1455.

25. Aquino JB, Sierra R and Montaldo LA. Diverse cellular origins of adult blood vascular endothelial cells. *Dev Biol*. 2021;477:117-132.
26. Anderson MJ, Pham VN, Vogel AM, Weinstein BM and Roman BL. Loss of unc45a precipitates arteriovenous shunting in the aortic arches. *Dev Biol*. 2008;318:258-67.
27. Li P, Pashmforoush M and Sucov HM. Mesodermal retinoic acid signaling regulates endothelial cell coalescence in caudal pharyngeal arch artery vasculogenesis. *Dev Biol*. 2012;361:116-24.
28. Paffett-Lugassy N, Singh R, Nevis KR, Guner-Ataman B, O'Loughlin E, Jahangiri L, Harvey RP, Burns CG and Burns CE. Heart field origin of great vessel precursors relies on nkx2.5-mediated vasculogenesis. *Nat Cell Biol*. 2013;15:1362-9.
29. Dobnikar L, Taylor AL, Chappell J, Oldach P, Harman JL, Oerton E, Dzierzak E, Bennett MR, Spivakov M and Jorgensen HF. Disease-relevant transcriptional signatures identified in individual smooth muscle cells from healthy mouse vessels. *Nat Commun*. 2018;9:4567.
30. Kim JB, Zhao Q, Nguyen T, Pjanic M, Cheng P, Wirka R, Travisano S, Nagao M, Kundu R and Quertermous T. Environment-Sensing Aryl Hydrocarbon Receptor Inhibits the Chondrogenic Fate of Modulated Smooth Muscle Cells in Atherosclerotic Lesions. *Circulation*. 2020;142:575-590.
31. Wirka RC, Wagh D, Paik DT, Pjanic M, Nguyen T, Miller CL, Kundu R, Nagao M, Coller J, Koyano TK, Fong R, Woo YJ, Liu B, Montgomery SB, Wu JC, Zhu K, Chang R, Alamprese M, Tallquist MD, Kim JB and Quertermous T. Atheroprotective roles of smooth muscle cell phenotypic modulation and the TCF21 disease gene as revealed by single-cell analysis. *Nat Med*. 2019;25:1280-1289.
32. Stuart T, Butler A, Hoffman P, Hafemeister C, Papalexi E, Mauck WM, 3rd, Hao Y, Stoeckius M, Smibert P and Satija R. Comprehensive Integration of Single-Cell Data. *Cell*. 2019;177:1888-1902 e21.
33. Cusanovich DA, Daza R, Adey A, Pliner HA, Christiansen L, Gunderson KL, Steemers FJ, Trapnell C and Shendure J. Multiplex single cell profiling of chromatin accessibility by combinatorial cellular indexing. *Science*. 2015;348:910-4.
34. Cusanovich DA, Reddington JP, Garfield DA, Daza RM, Aghamirzaie D, Marco-Ferreres R, Pliner HA, Christiansen L, Qiu X, Steemers FJ, Trapnell C, Shendure J and Furlong EEM. The cis-regulatory dynamics of embryonic development at single-cell resolution. *Nature*. 2018;555:538-542.
35. Schep AN, Wu B, Buenrostro JD and Greenleaf WJ. chromVAR: inferring transcription-factor-associated accessibility from single-cell epigenomic data. *Nat Methods*. 2017;14:975-978.
36. Liao Y, Smyth GK and Shi W. featureCounts: an efficient general purpose program for assigning sequence reads to genomic features. *Bioinformatics*. 2014;30:923-30.
37. Love MI, Huber W and Anders S. Moderated estimation of fold change and dispersion for RNA-seq data with DESeq2. *Genome Biol*. 2014;15:550.
38. Heinz S, Benner C, Spann N, Bertolino E, Lin YC, Laslo P, Cheng JX, Murre C, Singh H and Glass CK. Simple combinations of lineage-determining transcription factors prime cis-regulatory elements required for macrophage and B cell identities. *Mol Cell*. 2010;38:576-89.

39. McLean CY, Bristor D, Hiller M, Clarke SL, Schaar BT, Lowe CB, Wenger AM and Bejerano G. GREAT improves functional interpretation of cis-regulatory regions. *Nat Biotechnol*. 2010;28:495-501.
40. Liu J, Ren Y, Kang L and Zhang L. Overexpression of CCN3 inhibits inflammation and progression of atherosclerosis in apolipoprotein E-deficient mice. *PLoS One*. 2014;9:e94912.
41. Shimoyama T, Hiraoka S, Takemoto M, Koshizaka M, Tokuyama H, Tokuyama T, Watanabe A, Fujimoto M, Kawamura H, Sato S, Tsurutani Y, Saito Y, Perbal B, Koseki H and Yokote K. CCN3 inhibits neointimal hyperplasia through modulation of smooth muscle cell growth and migration. *Arterioscler Thromb Vasc Biol*. 2010;30:675-82.
42. Al Haj Zen A, Caligiuri G, Sainz J, Lemitre M, Demerens C and Lafont A. Decorin overexpression reduces atherosclerosis development in apolipoprotein E-deficient mice. *Atherosclerosis*. 2006;187:31-9.
43. Puig O, Yuan J, Stepaniants S, Zieba R, Zycband E, Morris M, Coulter S, Yu X, Menke J, Woods J, Chen F, Ramey DR, He X, O'Neill EA, Hailman E, Johns DG, Hubbard BK, Yee Lum P, Wright SD, Desouza MM, Plump A and Reiser V. A gene expression signature that classifies human atherosclerotic plaque by relative inflammation status. *Circ Cardiovasc Genet*. 2011;4:595-604.
44. Erdmann J, Kessler T, Munoz Venegas L and Schunkert H. A decade of genome-wide association studies for coronary artery disease: the challenges ahead. *Cardiovasc Res*. 2018;114:1241-1257.
45. Licht AH, Nubel T, Feldner A, Jurisch-Yaksi N, Marcello M, Demicheva E, Hu JH, Hartenstein B, Augustin HG, Hecker M, Angel P, Korff T and Schorpp-Kistner M. Junb regulates arterial contraction capacity, cellular contractility, and motility via its target Myl9 in mice. *J Clin Invest*. 2010;120:2307-18.
46. Harja E, Bucciarelli LG, Lu Y, Stern DM, Zou YS, Schmidt AM and Yan SF. Early growth response-1 promotes atherogenesis: mice deficient in early growth response-1 and apolipoprotein E display decreased atherosclerosis and vascular inflammation. *Circ Res*. 2004;94:333-9.
47. Li J, Adams LD, Wang X, Pabon L, Schwartz SM, Sane DC and Geary RL. Regulator of G protein signaling 5 marks peripheral arterial smooth muscle cells and is downregulated in atherosclerotic plaque. *J Vasc Surg*. 2004;40:519-28.
48. Daniel JM, Prock A, Dutzmann J, Sonnenschein K, Thum T, Bauersachs J and Sedding DG. Regulator of G-Protein Signaling 5 Prevents Smooth Muscle Cell Proliferation and Attenuates Neointima Formation. *Arterioscler Thromb Vasc Biol*. 2016;36:317-27.
49. Paloschi V, Kurtovic S, Folkersen L, Gomez D, Wagsater D, Roy J, Petrini J, Eriksson MJ, Caidahl K, Hamsten A, Liska J, Michel JB, Franco-Cereceda A and Eriksson P. Impaired splicing of fibronectin is associated with thoracic aortic aneurysm formation in patients with bicuspid aortic valve. *Arterioscler Thromb Vasc Biol*. 2011;31:691-7.
50. Soubeyrand S, Lau P, Nikpay M, Dang AT and McPherson R. Common Polymorphism That Protects From Cardiovascular Disease Increases Fibronectin Processing and Secretion. *Circ Genom Precis Med*. 2022:CIRCGEN121003428.

51. Azad AK, Chakrabarti S, Xu Z, Davidge ST and Fu Y. Coiled-coil domain containing 3 (CCDC3) represses tumor necrosis factor-alpha/nuclear factor kappaB-induced endothelial inflammation. *Cell Signal*. 2014;26:2793-800.
52. Lu Y, Haldar S, Croce K, Wang Y, Sakuma M, Morooka T, Wang B, Jeyaraj D, Gray SJ, Simon DI and Jain MK. Kruppel-like factor 15 regulates smooth muscle response to vascular injury--brief report. *Arterioscler Thromb Vasc Biol*. 2010;30:1550-2.
53. Lu Y, Zhang L, Liao X, Sangwung P, Prosdocimo DA, Zhou G, Votruba AR, Brian L, Han YJ, Gao H, Wang Y, Shimizu K, Weinert-Stein K, Khrestian M, Simon DI, Freedman NJ and Jain MK. Kruppel-like factor 15 is critical for vascular inflammation. *J Clin Invest*. 2013;123:4232-41.
54. Santiago FS, Ishii H, Shafi S, Khurana R, Kanellakis P, Bhindi R, Ramirez MJ, Bobik A, Martin JF, Chesterman CN, Zachary IC and Khachigian LM. Yin Yang-1 inhibits vascular smooth muscle cell growth and intimal thickening by repressing p21WAF1/Cip1 transcription and p21WAF1/Cip1-Cdk4-cyclin D1 assembly. *Circ Res*. 2007;101:146-55.
55. Santiago FS, Li Y, Zhong L, Raftery MJ, Lins L and Khachigian LM. Truncated YY1 interacts with BASP1 through a 339KLK341 motif in YY1 and suppresses vascular smooth muscle cell growth and intimal hyperplasia after vascular injury. *Cardiovasc Res*. 2021;117:2395-2406.
56. Li F, Tian F, Wang L, Williamson IK, Sharifi BG and Shah PK. Pleiotrophin (PTN) is expressed in vascularized human atherosclerotic plaques: IFN-{gamma}/JAK/STAT1 signaling is critical for the expression of PTN in macrophages. *FASEB J*. 2010;24:810-22.
57. Ress C, Paulweber M, Goebel G, Willeit K, Rufinatscha K, Strobl A, Salzmann K, Kedenko L, Tschoner A, Staudacher G, Iglseder B, Tilg H, Paulweber B and Kaser S. Circulating Wnt inhibitory factor 1 levels are associated with development of cardiovascular disease. *Atherosclerosis*. 2018;273:1-7.
58. Clemitson JR, Dixon RJ, Haines S, Bingham AJ, Patel BR, Hall L, Lo M, Sassard J, Charchar FJ and Samani NJ. Genetic dissection of a blood pressure quantitative trait locus on rat chromosome 1 and gene expression analysis identifies SPON1 as a novel candidate hypertension gene. *Circ Res*. 2007;100:992-9.
59. Prentice RL, Paczesny S, Aragaki A, Amon LM, Chen L, Pitteri SJ, McIntosh M, Wang P, Buson Busald T, Hsia J, Jackson RD, Rossouw JE, Manson JE, Johnson K, Eaton C and Hanash SM. Novel proteins associated with risk for coronary heart disease or stroke among postmenopausal women identified by in-depth plasma proteome profiling. *Genome Med*. 2010;2:48.
60. Yang X, Yang S, Xu H, Liu D, Zhang Y and Wang G. Superoxide Dismutase Gene Polymorphism is Associated With Ischemic Stroke Risk in the China Dali Region Han Population. *Neurologist*. 2021;26:27-31.
61. van de Laar IM, Oldenburg RA, Pals G, Roos-Hesselink JW, de Graaf BM, Verhagen JM, Hoedemaekers YM, Willemsen R, Severijnen LA, Venselaar H, Vriend G, Pattynama PM, Collee M, Majoor-Krakauer D, Poldermans D, Frohn-Mulder IM, Micha D, Timmermans J, Hilhorst-Hofstee Y, Bierma-Zeinstra SM, Willems PJ, Kros JM, Oei EH, Oostra BA, Wessels MW and Bertoli-Avella AM. Mutations in SMAD3 cause a

syndromic form of aortic aneurysms and dissections with early-onset osteoarthritis. *Nat Genet*. 2011;43:121-6.
62. Iyer D, Zhao Q, Wirka R, Naravane A, Nguyen T, Liu B, Nagao M, Cheng P, Miller CL, Kim JB, Pjanic M and Quertermous T. Coronary artery disease genes SMAD3 and TCF21 promote opposing interactive genetic programs that regulate smooth muscle cell differentiation and disease risk. *PLoS Genet*. 2018;14:e1007681.
63. Cui L, Chen SY, Lerbs T, Lee JW, Domizi P, Gordon S, Kim YH, Nolan G, Betancur P and Wernig G. Activation of JUN in fibroblasts promotes pro-fibrotic programme and modulates protective immunity. *Nat Commun*. 2020;11:2795.
64. Li Y, Ren P, Dawson A, Vasquez HG, Ageedi W, Zhang C, Luo W, Chen R, Li Y, Kim S, Lu HS, Cassis LA, Coselli JS, Daugherty A, Shen YH and LeMaire SA. Single-Cell Transcriptome Analysis Reveals Dynamic Cell Populations and Differential Gene Expression Patterns in Control and Aneurysmal Human Aortic Tissue. *Circulation*. 2020;142:1374-1388.
65. Goetze S, Kintscher U, Kaneshiro K, Meehan WP, Collins A, Fleck E, Hsueh WA and Law RE. TNFalpha induces expression of transcription factors c-fos, Egr-1, and Ets-1 in vascular lesions through extracellular signal-regulated kinases 1/2. *Atherosclerosis*. 2001;159:93-101.
66. Regard JB, Scheek S, Borbiev T, Lanahan AA, Schneider A, Demetriades AM, Hiemisch H, Barnes CA, Verin AD and Worley PF. Verge: a novel vascular early response gene. *J Neurosci*. 2004;24:4092-103.
67. Diaz-Canestro C, Bonetti NR, Wust P, Nageswaran V, Liberale L, Beer JH, Montecucco F, Luscher TF, Bohacek J and Camici GG. Apold1 deficiency associates with increased arterial thrombosis in vivo. *Eur J Clin Invest*. 2020;50:e13191.
68. Zhang J, Rojas S, Singh S, Musich PR, Gutierrez M, Yao Z, Thewke D and Jiang Y. Wnt2 Contributes to the Development of Atherosclerosis. *Front Cardiovasc Med*. 2021;8:751720.
69. Briot A, Jaroszewicz A, Warren CM, Lu J, Touma M, Rudat C, Hofmann JJ, Airik R, Weinmaster G, Lyons K, Wang Y, Kispert A, Pellegrini M and Iruela-Arispe ML. Repression of Sox9 by Jag1 is continuously required to suppress the default chondrogenic fate of vascular smooth muscle cells. *Dev Cell*. 2014;31:707-21.
70. Martos-Rodriguez CJ, Albarran-Juarez J, Morales-Cano D, Caballero A, MacGrogan D, de la Pompa JL, Carramolino L and Bentzon JF. Fibrous Caps in Atherosclerosis Form by Notch-Dependent Mechanisms Common to Arterial Media Development. *Arterioscler Thromb Vasc Biol*. 2021;41:e427-e439.
71. Traylor M, Tozer DJ, Croall ID, Lisiecka-Ford DM, Olorunda AO, Boncoraglio G, Dichgans M, Lemmens R, Rosand J, Rost NS, Rothwell PM, Sudlow CLM, Thijs V, Rutten-Jacobs L, Markus HS and International Stroke Genetics C. Genetic variation in PLEKHG1 is associated with white matter hyperintensities (n = 11,226). *Neurology*. 2019;92:e749-e757.
72. Wen H, Liu L, Zhan L, Liang D, Li L, Liu D, Sun W and Xu E. Neuroglobin mediates neuroprotection of hypoxic postconditioning against transient global cerebral ischemia in rats through preserving the activity of Na(+)/K(+) ATPases. *Cell Death Dis*. 2018;9:635.
73. Mukherjee K, Pingili AK, Singh P, Dhodi AN, Dutta SR, Gonzalez FJ and Malik KU. Testosterone Metabolite 6beta-Hydroxytestosterone Contributes to Angiotensin II-

Induced Abdominal Aortic Aneurysms in Apoe(-/-) Male Mice. *J Am Heart Assoc*. 2021;10:e018536.
74. Thirunavukkarasu S, Khan NS, Song CY, Ghafoor HU, Brand DD, Gonzalez FJ and Malik KU. Cytochrome P450 1B1 Contributes to the Development of Angiotensin II-Induced Aortic Aneurysm in Male Apoe(-/-) Mice. *Am J Pathol*. 2016;186:2204-2219.
75. Oettgen P. Regulation of vascular inflammation and remodeling by ETS factors. *Circ Res*. 2006;99:1159-66.
76. Schafer CM, Gurley JM, Kurylowicz K, Lin PK, Chen W, Elliott MH, Davis GE, Bhatti F and Griffin CT. An inhibitor of endothelial ETS transcription factors promotes physiologic and therapeutic vessel regression. *Proc Natl Acad Sci U S A*. 2020;117:26494-26502.
77. Zernecke A, Winkels H, Cochain C, Williams JW, Wolf D, Soehnlein O, Robbins CS, Monaco C, Park I, McNamara CA, Binder CJ, Cybulsky MI, Scipione CA, Hedrick CC, Galkina EV, Kyaw T, Ghosheh Y, Dinh HQ and Ley K. Meta-Analysis of Leukocyte Diversity in Atherosclerotic Mouse Aortas. *Circ Res*. 2020;127:402-426.
78. Li H, Zhang P, Zhang Q, Li C, Zou W, Chang Z, Cui CP and Zhang L. WWP2 is a physiological ubiquitin ligase for phosphatase and tensin homolog (PTEN) in mice. *J Biol Chem*. 2018;293:8886-8899.
79. Maurano MT, Humbert R, Rynes E, Thurman RE, Haugen E, Wang H, Reynolds AP, Sandstrom R, Qu H, Brody J, Shafer A, Neri F, Lee K, Kutyavin T, Stehling-Sun S, Johnson AK, Canfield TK, Giste E, Diegel M, Bates D, Hansen RS, Neph S, Sabo PJ, Heimfeld S, Raubitschek A, Ziegler S, Cotsapas C, Sotoodehnia N, Glass I, Sunyaev SR, Kaul R and Stamatoyannopoulos JA. Systematic localization of common disease-associated variation in regulatory DNA. *Science*. 2012;337:1190-5.
80. Chen Y, Xiao D, Zhang L, Cai CL, Li BY and Liu Y. The Role of Tbx20 in Cardiovascular Development and Function. *Front Cell Dev Biol*. 2021;9:638542.
81. Koyama S, Ito K, Terao C, Akiyama M, Horikoshi M, Momozawa Y, Matsunaga H, Ieki H, Ozaki K, Onouchi Y, Takahashi A, Nomura S, Morita H, Akazawa H, Kim C, Seo JS, Higasa K, Iwasaki M, Yamaji T, Sawada N, Tsugane S, Koyama T, Ikezaki H, Takashima N, Tanaka K, Arisawa K, Kuriki K, Naito M, Wakai K, Suna S, Sakata Y, Sato H, Hori M, Sakata Y, Matsuda K, Murakami Y, Aburatani H, Kubo M, Matsuda F, Kamatani Y and Komuro I. Population-specific and trans-ancestry genome-wide analyses identify distinct and shared genetic risk loci for coronary artery disease. *Nat Genet*. 2020;52:1169-1177.
82. Sakaue S, Kanai M, Tanigawa Y, Karjalainen J, Kurki M, Koshiba S, Narita A, Konuma T, Yamamoto K, Akiyama M, Ishigaki K, Suzuki A, Suzuki K, Obara W, Yamaji K, Takahashi K, Asai S, Takahashi Y, Suzuki T, Shinozaki N, Yamaguchi H, Minami S, Murayama S, Yoshimori K, Nagayama S, Obata D, Higashiyama M, Masumoto A, Koretsune Y, FinnGen, Ito K, Terao C, Yamauchi T, Komuro I, Kadowaki T, Tamiya G, Yamamoto M, Nakamura Y, Kubo M, Murakami Y, Yamamoto K, Kamatani Y, Palotie A, Rivas MA, Daly MJ, Matsuda K and Okada Y. A cross-population atlas of genetic associations for 220 human phenotypes. *Nat Genet*. 2021;53:1415-1424.
83. Warren HR, Evangelou E, Cabrera CP, Gao H, Ren M, Mifsud B, Ntalla I, Surendran P, Liu C, Cook JP, Kraja AT, Drenos F, Loh M, Verweij N, Marten J, Karaman I, Lepe MP, O'Reilly PF, Knight J, Snieder H, Kato N, He J, Tai ES, Said MA, Porteous D, Alver M, Poulter N, Farrall M, Gansevoort RT, Padmanabhan S, Magi R,

Stanton A, Connell J, Bakker SJ, Metspalu A, Shields DC, Thom S, Brown M, Sever P, Esko T, Hayward C, van der Harst P, Saleheen D, Chowdhury R, Chambers JC, Chasman DI, Chakravarti A, Newton-Cheh C, Lindgren CM, Levy D, Kooner JS, Keavney B, Tomaszewski M, Samani NJ, Howson JM, Tobin MD, Munroe PB, Ehret GB, Wain LV, International Consortium of Blood Pressure GA, Consortium B, Lifelines Cohort S, Understanding Society Scientific g, Consortium CHDE, Exome BPC, Consortium TDG, Go TDC, Cohorts for H, Ageing Research in Genome Epidemiology BPEC, International Genomics of Blood Pressure C and group UKBCCBw. Genome-wide association analysis identifies novel blood pressure loci and offers biological insights into cardiovascular risk. *Nat Genet*. 2017;49:403-415.
84. Benjamins JW, Yeung MW, van de Vegte YJ, Said MA, van der Linden T, Ties D, Juarez-Orozco LE, Verweij N and van der Harst P. Genomic insights in ascending aortic size and distensibility. *EBioMedicine*. 2022;75:103783.
85. Takeuchi F, Akiyama M, Matoba N, Katsuya T, Nakatochi M, Tabara Y, Narita A, Saw WY, Moon S, Spracklen CN, Chai JF, Kim YJ, Zhang L, Wang C, Li H, Li H, Wu JY, Dorajoo R, Nierenberg JL, Wang YX, He J, Bennett DA, Takahashi A, Momozawa Y, Hirata M, Matsuda K, Rakugi H, Nakashima E, Isono M, Shirota M, Hozawa A, Ichihara S, Matsubara T, Yamamoto K, Kohara K, Igase M, Han S, Gordon-Larsen P, Huang W, Lee NR, Adair LS, Hwang MY, Lee J, Chee ML, Sabanayagam C, Zhao W, Liu J, Reilly DF, Sun L, Huo S, Edwards TL, Long J, Chang LC, Chen CH, Yuan JM, Koh WP, Friedlander Y, Kelly TN, Bin Wei W, Xu L, Cai H, Xiang YB, Lin K, Clarke R, Walters RG, Millwood IY, Li L, Chambers JC, Kooner JS, Elliott P, van der Harst P, International Genomics of Blood Pressure C, Chen Z, Sasaki M, Shu XO, Jonas JB, He J, Heng CK, Chen YT, Zheng W, Lin X, Teo YY, Tai ES, Cheng CY, Wong TY, Sim X, Mohlke KL, Yamamoto M, Kim BJ, Miki T, Nabika T, Yokota M, Kamatani Y, Kubo M and Kato N. Interethnic analyses of blood pressure loci in populations of East Asian and European descent. *Nat Commun*. 2018;9:5052.
86. Kichaev G, Bhatia G, Loh PR, Gazal S, Burch K, Freund MK, Schoech A, Pasaniuc B and Price AL. Leveraging Polygenic Functional Enrichment to Improve GWAS Power. *Am J Hum Genet*. 2019;104:65-75.
87. Roselli C, Chaffin MD, Weng LC, Aeschbacher S, Ahlberg G, Albert CM, Almgren P, Alonso A, Anderson CD, Aragam KG, Arking DE, Barnard J, Bartz TM, Benjamin EJ, Bihlmeyer NA, Bis JC, Bloom HL, Boerwinkle E, Bottinger EB, Brody JA, Calkins H, Campbell A, Cappola TP, Carlquist J, Chasman DI, Chen LY, Chen YI, Choi EK, Choi SH, Christophersen IE, Chung MK, Cole JW, Conen D, Cook J, Crijns HJ, Cutler MJ, Damrauer SM, Daniels BR, Darbar D, Delgado G, Denny JC, Dichgans M, Dorr M, Dudink EA, Dudley SC, Esa N, Esko T, Eskola M, Fatkin D, Felix SB, Ford I, Franco OH, Geelhoed B, Grewal RP, Gudnason V, Guo X, Gupta N, Gustafsson S, Gutmann R, Hamsten A, Harris TB, Hayward C, Heckbert SR, Hernesniemi J, Hocking LJ, Hofman A, Horimoto A, Huang J, Huang PL, Huffman J, Ingelsson E, Ipek EG, Ito K, Jimenez-Conde J, Johnson R, Jukema JW, Kaab S, Kahonen M, Kamatani Y, Kane JP, Kastrati A, Kathiresan S, Katschnig-Winter P, Kavousi M, Kessler T, Kietselaer BL, Kirchhof P, Kleber ME, Knight S, Krieger JE, Kubo M, Launer LJ, Laurikka J, Lehtimaki T, Leineweber K, Lemaitre RN, Li M, Lim HE, Lin HJ, Lin H, Lind L, Lindgren CM, Lokki ML, London B, Loos RJF, Low SK, Lu Y, Lyytikainen LP, Macfarlane PW, Magnusson PK, Mahajan A, Malik R, Mansur AJ, Marcus GM, Margolin L, Margulies KB, Marz W,

McManus DD, Melander O, Mohanty S, Montgomery JA, Morley MP, Morris AP, Muller-Nurasyid M, Natale A, Nazarian S, Neumann B, Newton-Cheh C, Niemeijer MN, Nikus K, Nilsson P, Noordam R, Oellers H, Olesen MS, Orho-Melander M, Padmanabhan S, Pak HN, Pare G, Pedersen NL, Pera J, Pereira A, Porteous D, Psaty BM, Pulit SL, Pullinger CR, Rader DJ, Refsgaard L, Ribases M, Ridker PM, Rienstra M, Risch L, Roden DM, Rosand J, Rosenberg MA, Rost N, Rotter JI, Saba S, Sandhu RK, Schnabel RB, Schramm K, Schunkert H, Schurman C, Scott SA, Seppala I, Shaffer C, Shah S, Shalaby AA, Shim J, Shoemaker MB, Siland JE, Sinisalo J, Sinner MF, Slowik A, Smith AV, Smith BH, Smith JG, Smith JD, Smith NL, Soliman EZ, Sotoodehnia N, Stricker BH, Sun A, Sun H, Svendsen JH, Tanaka T, Tanriverdi K, Taylor KD, Teder-Laving M, Teumer A, Theriault S, Trompet S, Tucker NR, Tveit A, Uitterlinden AG, Van Der Harst P, Van Gelder IC, Van Wagoner DR, Verweij N, Vlachopoulou E, Volker U, Wang B, Weeke PE, Weijs B, Weiss R, Weiss S, Wells QS, Wiggins KL, Wong JA, Woo D, Worrall BB, Yang PS, Yao J, Yoneda ZT, Zeller T, Zeng L, Lubitz SA, Lunetta KL and Ellinor PT. Multi-ethnic genome-wide association study for atrial fibrillation. *Nat Genet*. 2018;50:1225-1233.

88. Acharya A, Baek ST, Huang G, Eskiocak B, Goetsch S, Sung CY, Banfi S, Sauer MF, Olsen GS, Duffield JS, Olson EN and Tallquist MD. The bHLH transcription factor Tcf21 is required for lineage-specific EMT of cardiac fibroblast progenitors. *Development*. 2012;139:2139-49.

89. Fardi M, Alivand M, Baradaran B, Farshdousti Hagh M and Solali S. The crucial role of ZEB2: From development to epithelial-to-mesenchymal transition and cancer complexity. *J Cell Physiol*. 2019.

90. Shi H, Zhang C, Pasupuleti V, Hu X, Prosdocimo DA, Wu W, Qing Y, Wu S, Mohammad H, Gerson SL, Perbal B, Klenotic PA, Dong N and Lin Z. CCN3 Regulates Macrophage Foam Cell Formation and Atherosclerosis. *Am J Pathol*. 2017;187:1230-1237.

91. Aune D, Schlesinger S, Norat T and Riboli E. Tobacco smoking and the risk of abdominal aortic aneurysm: a systematic review and meta-analysis of prospective studies. *Sci Rep*. 2018;8:14786.

92. Port JL, Yamaguchi K, Du B, De Lorenzo M, Chang M, Heerdt PM, Kopelovich L, Marcus CB, Altorki NK, Subbaramaiah K and Dannenberg AJ. Tobacco smoke induces CYP1B1 in the aerodigestive tract. *Carcinogenesis*. 2004;25:2275-81.

93. Xie W, Ke Y, You Q, Li J, Chen L, Li D, Fang J, Chen X, Zhou Y, Chen L and Hong H. Single-Cell RNA Sequencing and Assay for Transposase-Accessible Chromatin Using Sequencing Reveals Cellular and Molecular Dynamics of Aortic Aging in Mice. *Arterioscler Thromb Vasc Biol*. 2022;42:156-171.

Figures and Figure Legends

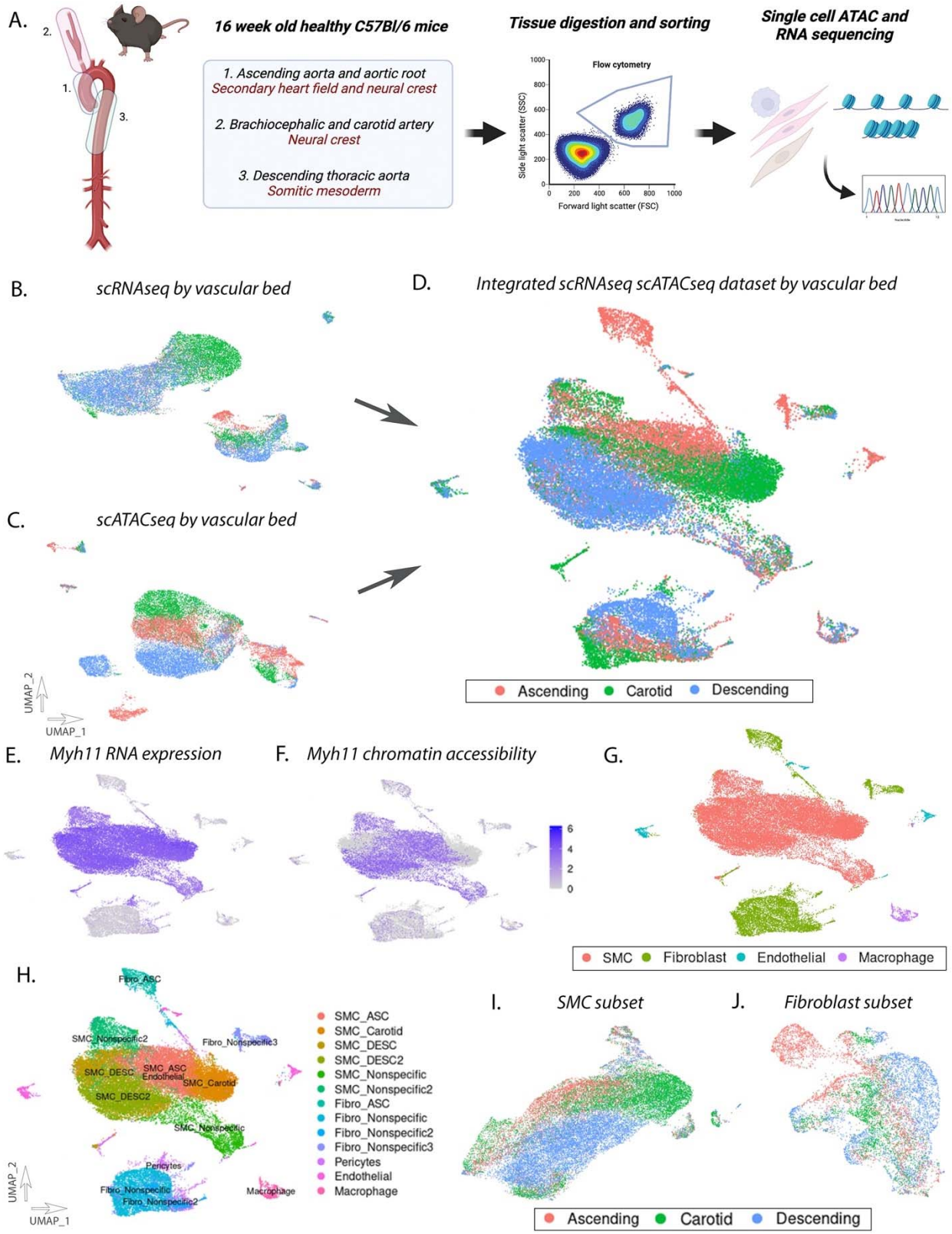

Figure 1. Transcriptomic and epigenomic landscape of single vascular cells. Single cell RNA seq (scRNAseq) and single cell ATAC seq (scATACseq) was performed on vascular tissue in adult healthy mice C57Bl/6) in three vascular beds (aortic root/ascending aorta, brachiocephalic/carotid artery, descending thoracic aorta)(Panel A). UMAP of scRNAseq data (Panel B) and scATACseq data (Panel C) show prominent differentiation of cells by vascular bed that is further characterized by integrated dataset and UMAP visualization (Panel D). Significant concordance is seen between RNA expression and gene chromatin accessibility (Panel E – RNA expression *Myh11*; Panel F — chromatin accessibility gene score, *Myh11*). Expression of canonical genes is used to differentiate cell populations into the 4 major cell types of the vascular wall — smooth muscle cells (SMCs), fibroblasts, endothelial cells, and macrophage cells and to display with UMAP visualization (Panel G). Unbiased cell clustering reveals SMC and fibroblasts to largely differentiate by vascular bed but also reveal additional nonspecific clusters composed of cells from each vascular bed (Panel H). Subsetting and UMAP visualization of integrated data for SMCs (Panel I) and fibroblasts (Panel J) show significant differentiation of cells by vascular bed.

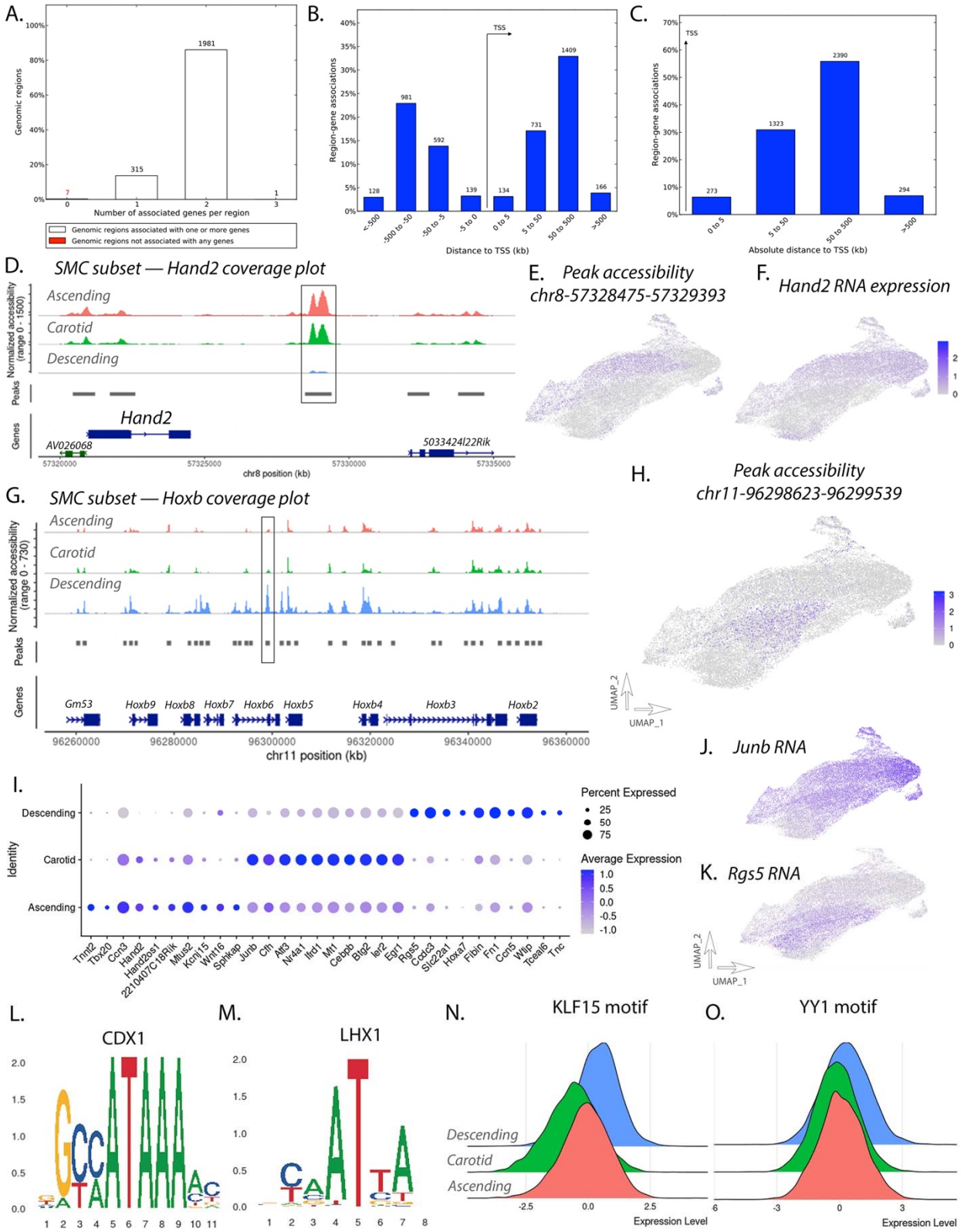
A.
Genomic regions
Number of associated genes per region
Genomic regions associated with one or more genes
Genomic regions not associated with any genes
B.
Region-gene associations
Distance to TSS (kb)
TSS
C.
Region-gene associations
Absolute distance to TSS (kb)
D.
SMC subset — Hand2 coverage plot
Ascending
Carotid
Descending
Normalized accessibility (range 0 - 1500)
Peaks
Genes
Hand2
AV026068
5033424I22Rik
chr8 position (kb)
E.
Peak accessibility
chr8-57328475-57329393
F.
Hand2 RNA expression
G.
SMC subset — Hoxb coverage plot
Normalized accessibility (range 0 - 730)
Gm53
Hoxb9
Hoxb8
Hoxb7
Hoxb6
Hoxb5
Hoxb4
Hoxb3
Hoxb2
chr11 position (kb)
H.
Peak accessibility
chr11-96298623-96299539
UMAP_2
UMAP_1
I.
Identity
Descending
Carotid
Ascending
Percent Expressed
Average Expression
J.
Junb RNA
K.
Rgs5 RNA
L.
CDX1
M.
LHX1
N.
KLF15 motif
O.
YY1 motif
Expression Level

Figure 2. SMC subset analysis reveals differential chromatin peak accessibility, gene expression, and transcription factor motif accessibility between vascular beds. 2304 peaks are found to be differentially accessible between ascending aorta and descending aorta SMCs, and peak to gene analysis using GREAT shows the majority of peaks associate with 2 genes (Panel A). Analysis of the distance from peak to associated gene TSSs (Panels B and C) show the majority to be downstream of the TSS with roughly 10% of peaks being within 5kb of the TSS of a gene. Accessibility for peak Chr8-57328475-57329393, 7951bp downstream from the TSS for *Hand2* (heart and neural crest derivatives expressed 2) is higher in ascending and carotid SMCs (Coverage plot — Panel D), feature plot of peak Chr8-57328475-57329393 (Panel E) corresponds to *Hand2* RNA expression (Panel F). Coverage plot of peak chr11-96298623-96299539 shows marked increased accessibility within descending aorta SMCs (Panel G) and feature plot of chr11-96298623-96299539 demonstrates a pattern distinct to descending aorta SMCs (Panel H). Dot plot of RNA expression of top 10 genes per vascular bed highlight development and disease relevant genes (Panel I), including *Junb* (RNA feature plot — Panel J) and *Rgs5* (RNA feature plot — Panel K). Evaluation of transcription factor (TF) motif accessibility using ChromVAR reveals specific developmental and disease relevant TFs to have differential accessibility, notably homeobox family TFs with higher accessibility within the descending aorta SMCs (caudal type homeobox, CDX1 — Panel L), LIM homeobox 1 (LHX1 — Panel M), KLF15 (Panel N), and YY1 (Panel O).

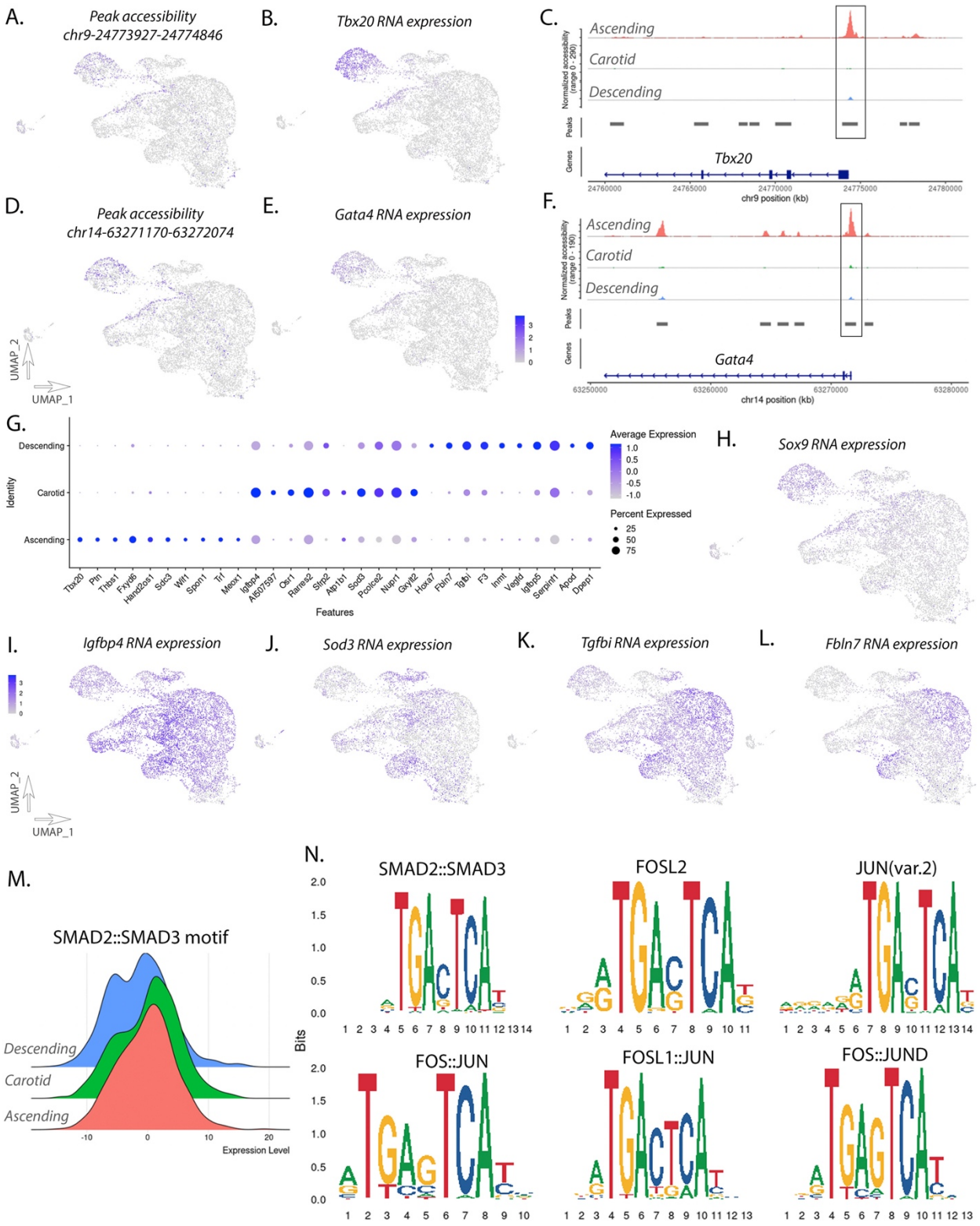
A.
Peak accessibility
chr9-24773927-24774846
B.
Tbx20 RNA expression
C.
Ascending
Carotid
Descending
Normalized accessibility (range 0 - 290)
Peaks
Genes
Tbx20
24760000
24765000
24770000
24775000
24780000
chr9 position (kb)
D.
Peak accessibility
chr14-63271170-63272074
E.
Gata4 RNA expression
F.
Ascending
Carotid
Descending
Normalized accessibility (range 0 - 190)
Peaks
Genes
Gata4
63250000
63260000
63270000
63280000
chr14 position (kb)
UMAP_2
UMAP_1
G.
Descending
Carotid
Ascending
Identity
Average Expression
Percent Expressed
Features
Tbx20
Pitx
Thbs1
Fxyd6
Hand2os1
Sdc3
Wif1
Spon1
Tnf
Meox1
Igfbp4
AI607597
Osr1
Rarres2
Sfrp2
Atp1b1
Sod3
Pcolce2
Nupr1
Gxylt2
Hoxa7
Fbln7
Tgfbi
F3
Inmt
Vegfd
Igfbp5
Serpinf1
Apod
Dpep1
H.
Sox9 RNA expression
I.
Igfbp4 RNA expression
J.
Sod3 RNA expression
K.
Tgfbi RNA expression
L.
Fbln7 RNA expression
M.
SMAD2::SMAD3 motif
Descending
Carotid
Ascending
Expression Level
N.
SMAD2::SMAD3
FOSL2
JUN(var.2)
FOS::JUN
FOSL1::JUN
FOS::JUND
Bits

Figure 3. Fibroblast subset analysis reveals vascular bed specific enhancers for developmental and disease genes. Differential peak accessibility analysis identifies 2,140 differentially peaks between ascending and descending aorta fibroblasts, notably peak chr9-24773927-24774846 has higher accessibility within the ascending aorta (Feature plot — Panel A), corresponds to higher expression of *Tbx20* (RNA feature plot — Panel B), and lies 103 bp away from the TSS for *Tbx20* (Coverage plot — Panel C). Similarly, peak chr14-63271170-63272074 has higher accessibility within the ascending aorta (Feature plot — Panel D), corresponds to *Gata4* expression (RNA feature plot — Panel E), and lies 87 bp away from the TSS for *Gata4* (Panel F). Dot plot analysis of RNA expression of the top 10 differentially expressed genes highlights developmental and disease relevant genes within fibroblasts (Panel G), notably *Sox9* with higher expression within the ascending fibroblasts (Panel H), *Igfbp4* and *Sod3* with higher expression within the carotid fibroblasts (Panels I and J), and *Tgfbi* and *Fbln7* with higher expression in the descending fibroblasts (Panels K and L). Transcription factor (TF) motif accessibility analysis using ChromVAR identified specific TFs to have differential motif accessibility, including SMAD2::SMAD3 to have higher accessibility within the ascending aorta (Panels M and N), along with the top 6 motifs including FOS and JUN related motifs which have higher accessibility within the ascending aorta (FOSL2, JUN, FOS::JUN, FOSL1::JUN, and FOS::JUND — Panel N).

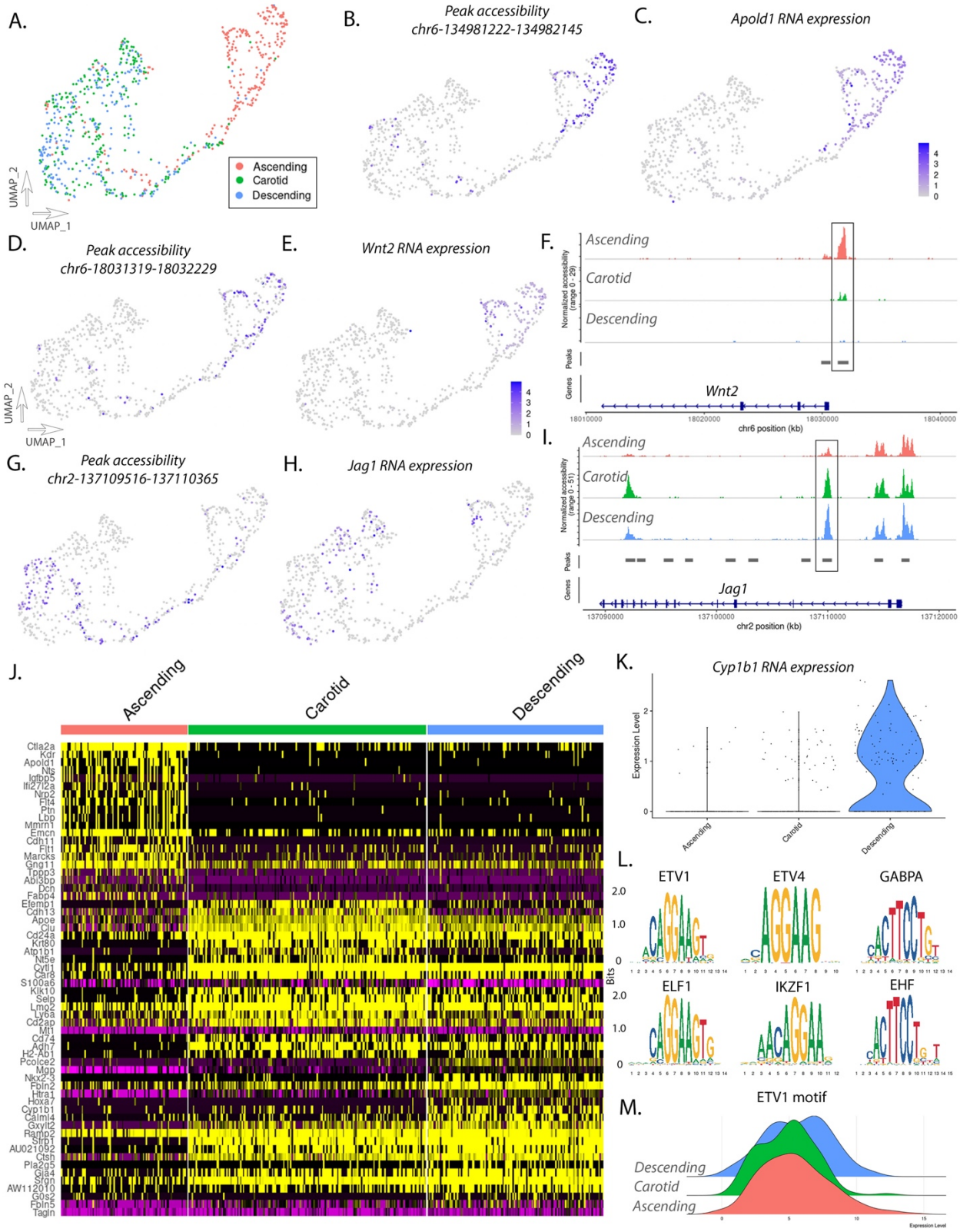
A.
Ascending
Carotid
Descending
UMAP_2
UMAP_1
B.
Peak accessibility
chr6-134981222-134982145
C.
Apold1 RNA expression
D.
Peak accessibility
chr6-18031319-18032229
E.
Wnt2 RNA expression
F.
Ascending
Carotid
Descending
Normalized accessibility (range 0 - 29)
Peaks
Genes
Wnt2
chr6 position (kb)
G.
Peak accessibility
chr2-137109516-137110365
H.
Jag1 RNA expression
I.
Ascending
Carotid
Descending
Normalized accessibility (range 0 - 51)
Peaks
Genes
Jag1
chr2 position (kb)
J.
Ascending
Carotid
Descending
K.
Cyp1b1 RNA expression
Expression Level
L.
ETV1
ETV4
GABPA
ELF1
IKZF1
EHF
Bits
M.
ETV1 motif
Descending
Carotid
Ascending
Expression Level

Figure 4. Endothelial cell subset analysis identifies differentially accessible chromatin peaks and differential transcription factor (TF) motif accessibility. UMAP visualization of integrated scRNAseq/scATACseq data of endothelial cells demonstrates separation of endothelial cells from the ascending aorta, with modest separation between carotid and descending endothelial cells (Panel A). 223 differentially accessible peaks were identified between ascending and descending endothelial cells, a top peak with increased accessibility in the ascending endothelial cells is chr6-134981222-134982145 which lies 34bp upstream of the TSS of *Apold1* (Panel B), which correlates to *Apold1* RNA expression (Panel C). Similarly, accessibility of peak chr6-18031319-18032229 is greater in ascending endothelial cells (Panel D), which correlates to *Wnt2* RNA expression (Panel E) and lies 1189bp downstream of the TSS for *Wnt2* (Panel F). Increased accessibility of peak chr2-137109516-137110365 is seen in descending endothelial cells (Panel G), which correlates to increased RNA expression of *Jag1* (Panel H), and lies 6703bp upstream of the TSS for *Jag1* (Panel I). Heatmap of endothelial cells by vascular bed reveals top differentially expressed genes by RNA (Panel J). *Cyp1b1* has higher expression within descending aorta endothelial cells (Violin Plot — Panel K). Differential TF motif accessibility identifies ETS (E26 Transformation-specific Sequence) family of TFs to have higher motif accessibility in the descending aorta endothelial cells (Panels L and M).

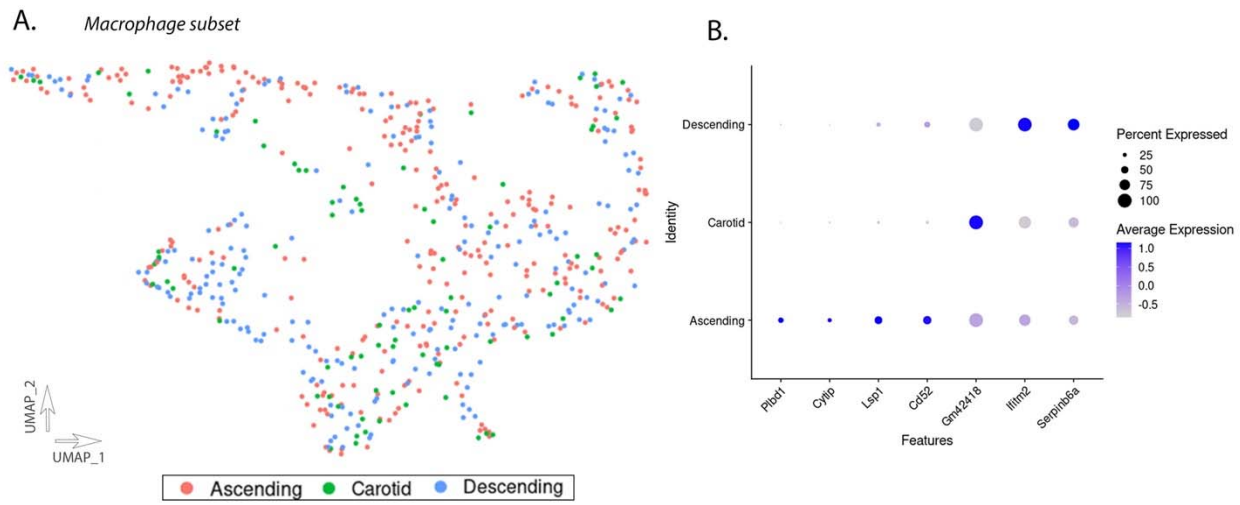

Figure 5. Single cell transcriptomic and epigenomic analysis of macrophage cells reveals notable homogeneity between vascular beds. UMAP visualization of macrophage cell subset highlights striking similarity between vascular beds with nearly unanimous overlap (Panel A). No differential chromatin peaks were identified, with only 7 genes found to have differential expression between by scRNAseq (Dot plot — Panel B).

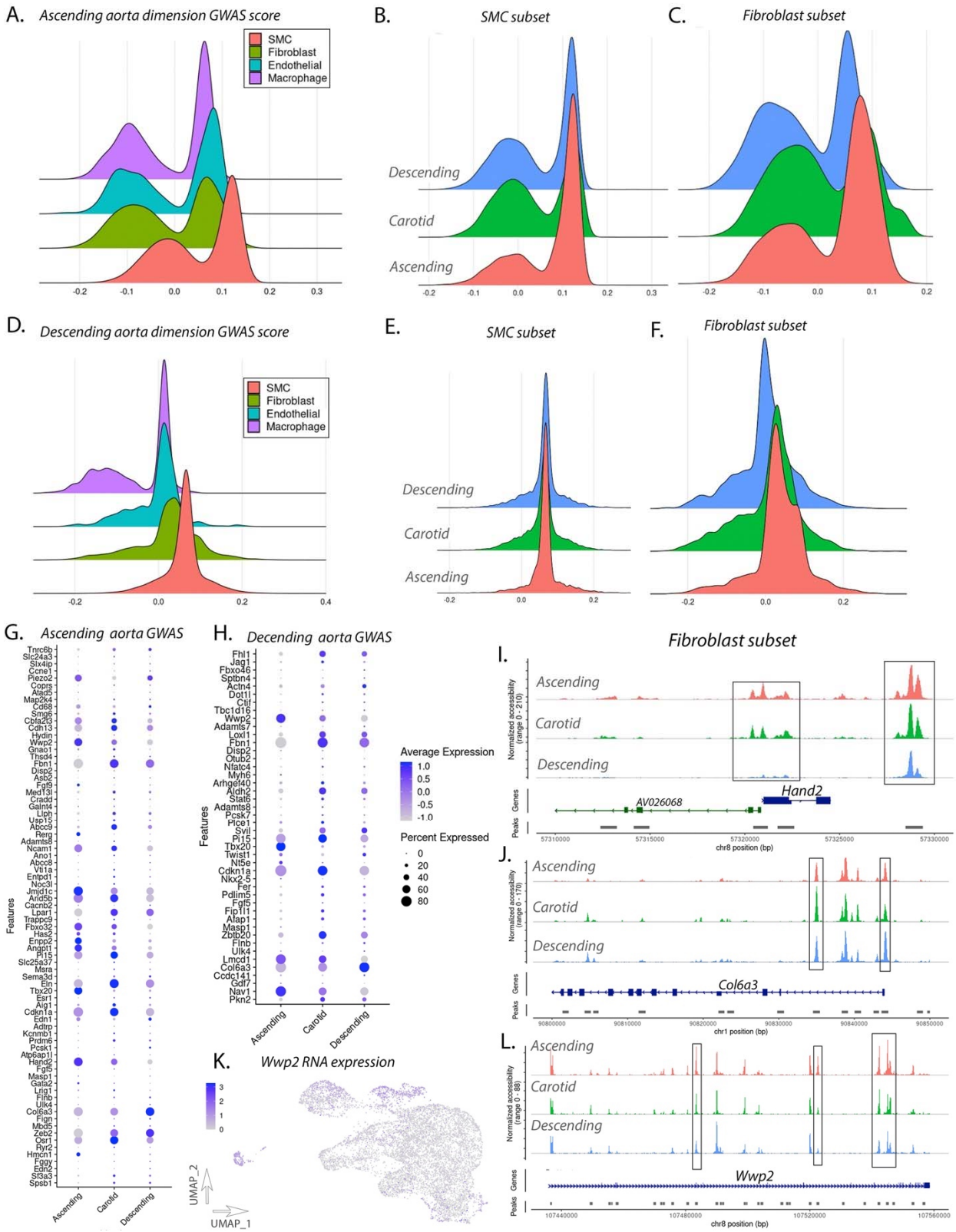
A.
Ascending aorta dimension GWAS score
SMC
Fibroblast
Endothelial
Macrophage
B.
SMC subset
C.
Fibroblast subset
Descending
Carotid
Ascending
D.
Descending aorta dimension GWAS score
E.
SMC subset
F.
Fibroblast subset
G.
Ascending aorta GWAS
Features
Ascending
Carotid
Descending
H.
Decending aorta GWAS
Average Expression
Percent Expressed
I.
Fibroblast subset
Normalized accessibility
Genes
Peaks
AV026068
Hand2
chr8 position (bp)
J.
Col6a3
chr1 position (bp)
K.
Wwp2 RNA expression
UMAP_1
UMAP_2
L.
Wwp2
chr8 position (bp)

Figure 6. GWAS score analysis for aortic dimension identifies cell type and vascular bed specific scores for GWAS genes. Aortic dimension scores based on loci from Pirruccello et al. (2022) show that an ascending aorta dimension score is highest in SMCs and lowest for macrophage cells (Panel A). There is no difference in ascending aorta dimension score in SMCs between vascular beds (Panel B) but fibroblasts have a higher score in the ascending aorta (Panel C), suggesting vascular bed specific GWAS gene expression influencing aortic dimension. Descending aorta dimension score is highest in SMCs and lowest in macrophage cells (Panel D), and similarly, there is no change in descending aorta dimension score in SMCs across vascular beds (Panel E), but an increase in score in ascending fibroblasts (Panel F). Evaluation of each gene within the ascending dimension score (Dot plot — Panel G) and the descending dimension score (Dot plot — Panel H), highlights specific genes with vascular bed specific expression. Notably, *Hand2* is a GWAS aortic dimension gene, has higher expression in the ascending aorta, and coverage plot of this region demonstrates increased chromatin accessibility in ascending fibroblasts (Panel I). *Col6a3* is a GWAS dimension gene which has higher expression in the descending aorta, and coverage plot shows increased chromatin accessibility in descending fibroblasts (Panel J). *Wwp2* is an aortic dimension GWAS gene with higher expression in the ascending aorta (Feature plot — Panel K), and increased chromatin accessibility in the ascending aorta (Coverage plot — Panel L).

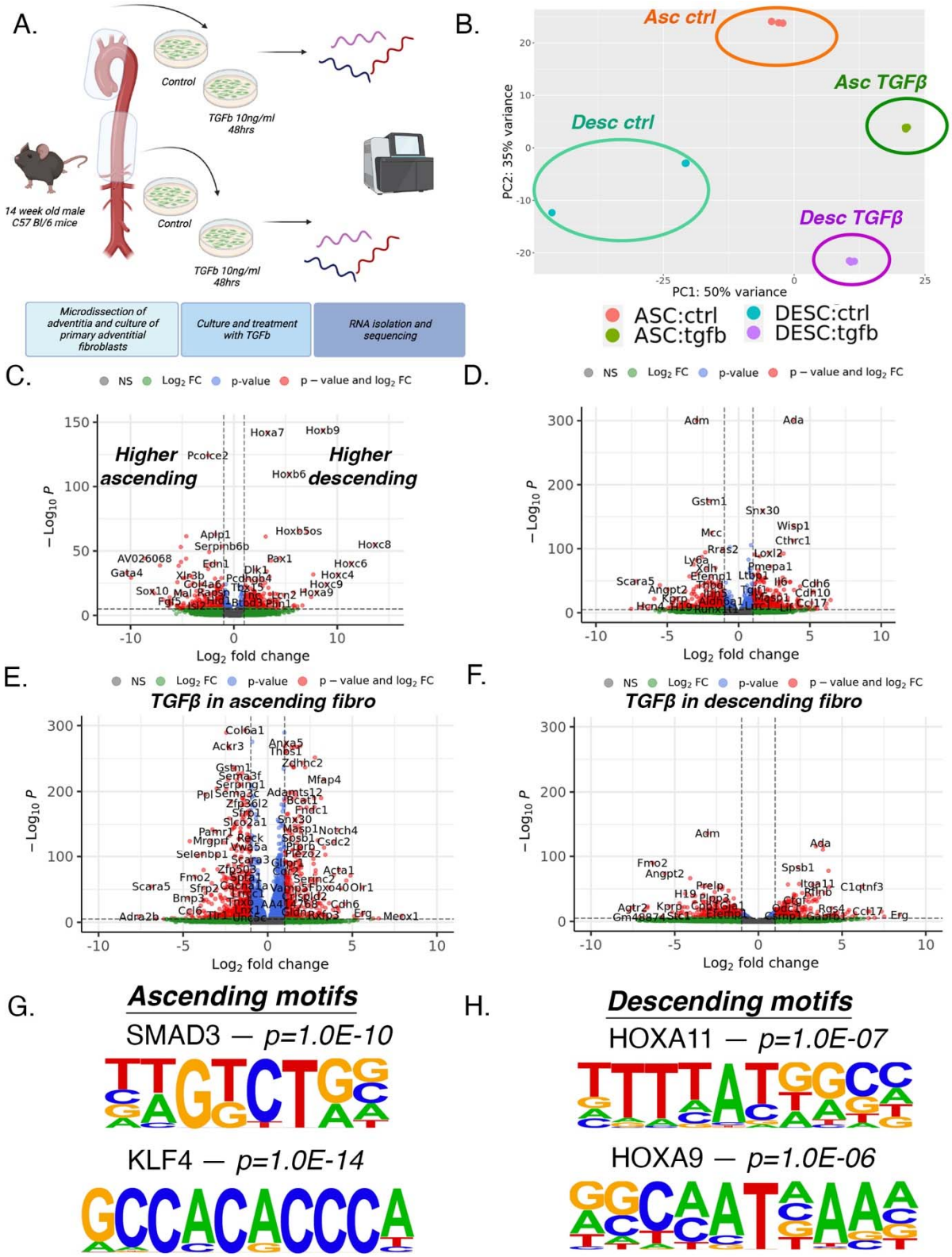
A.
Control
TGFb 10ng/ml
48hrs
14 week old male
C57 Bl/6 mice
Control
TGFb 10ng/ml
48hrs
Microdissection of adventitia and culture of primary adventitial fibroblasts
Culture and treatment with TGFb
RNA isolation and sequencing
B.
Asc ctrl
Asc TGFβ
Desc ctrl
Desc TGFβ
PC2: 35% variance
PC1: 50% variance
ASC:ctrl
ASC:tgfb
DESC:ctrl
DESC:tgfb
C.
NS
Log2 FC
p-value
p – value and log2 FC
Higher ascending
Higher descending
Log2 fold change
D.
NS
Log2 FC
p-value
p – value and log2 FC
Log2 fold change
E.
NS
Log2 FC
p-value
p – value and log2 FC
TGFβ in ascending fibro
Log2 fold change
F.
NS
Log2 FC
p-value
p – value and log2 FC
TGFβ in descending fibro
Log2 fold change
G.
Ascending motifs
SMAD3 — p=1.0E-10
KLF4 — p=1.0E-14
H.
Descending motifs
HOXA11 — p=1.0E-07
HOXA9 — p=1.0E-06

Figure 7. Primary adventitial fibroblasts retain vascular bed specific transcriptomic features by vascular bed following *in vitro* culture and reveal vascular bed specific response to TGFβ. Primary adventitial fibroblasts were isolated and cultured and subsequently treated with TGFβ prior to RNA isolation and RNA sequencing (Panel A). Principal component analysis (PCA) shows distinct transcriptomic patterns by vascular bed and TGFβ treatment (Panel B). Differential gene expression (DEG) analysis of all samples by vascular bed reveal evidence of persistent differential gene expression by vascular bed following *in vitro* culture (Panel C). DEG analysis of all samples by TGFβ treatment (Panel D) show distinct primary fibroblast response to TGFβ, an effect that is markedly higher in ascending fibroblasts (Panel E) than in descending fibroblasts (Panel F). Evaluation of transcription factor motif enrichment of genes with increased expression in ascending fibroblasts (Panel G) reveal key TFs governing response to TGFβ and phenotypic modulation, including SMAD3 and KLF4. TF motif enrichment of genes with increased expression in descending fibroblasts (Panel H) highlight HOX family of transcription factors, including HOXA11 and HOXA9.